JBC Papers in Press. Published on June 22, 2017 as Manuscript M117.796425
The latest version is at http://www.jbc.org/cgi/doi/10.1074/jbc.M117.796425

Saccharomyces cerevisiae Red1 protein exhibits nonhomologous DNA end–joining activity and potentiates Hop1 promoted pairing of double-stranded DNA

Rucha Kshirsagar, Indrajeet Ghodke and Kalappa Muniyappa[1*]
Department of Biochemistry, Indian Institute of Science
Bangalore 560012, India

Running title: Yeast Red1 is a structure-selective DNA binding protein

*To whom correspondence should be addressed: K. Muniyappa; E-mail: kmbc@biochem.iisc.ernet.in, Tel.: +91 80 2293 2235/2360 0278, Fax: +91 80 2360 0814/0683

Key words: Synaptonemal complex; Hop1 protein; Red1 protein; Holliday junction; DNA pairing; DNA end joining; DNA bridging; meiotic recombination

ABSTRACT

Elucidation of the function of synaptonemal complex (SC) in *Saccharomyces cerevisiae* has mainly focused on *in vivo* analysis of recombination-defective meiotic mutants. Consequently, significant gaps remain in the mechanistic understanding of the activities of various SC proteins and the functional relationships among them. *S. cerevisiae* Hop1 and Red1 are essential structural components of the SC axial/lateral elements. Previous studies have demonstrated that Hop1 is a structure-selective DNA-binding protein exhibiting high affinity for the Holliday junction and promoting DNA bridging, condensation and pairing between double-stranded DNA molecules. However, the exact mode of action of Red1 remains unclear, although it is known to interact with Hop1 and to suppress the spore viability defects of *hop1* mutant alleles. Here, we report the purification and functional characterization of the full-length Red1 protein. Our results revealed that Red1 forms a stable complex with Hop1 *in vitro* and provided quantitative insights into their physical interactions. Mechanistically, Red1 preferentially associated with the Holliday junction and three-way junction rather than with single- or double-stranded DNA with overhangs. Although Hop1 and Red1 exhibited similar binding affinities toward several DNA substrates, the two proteins displayed some significant differences. Notably, Red1, by itself, lacked DNA-pairing ability; however, it potentiated Hop1 promoted intermolecular pairing between double-stranded DNA molecules. Moreover, Red1 exhibited non-homologous DNA end-joining activity, thus revealing an unexpected role for Red1 in recombination-based DNA repair. Collectively, this study presents the first direct insights into the Red1's mode of action and into the mechanism underlying its role in chromosome synapsis and recombination.

INTRODUCTION

Meiosis is a specialized form of cell division during which the diploid cells undergo a single round of DNA replication followed by two rounds of chromosome segregation to produce haploid gametes. During meiosis I, homologous chromosomes, one from each parent, pair up and exchange genetic material by crossing over (1, 2). In most eukaryotes, a meiosis-specific, dense, proteinaceous structure, called the synaptonemal complex (SC), is necessary for crossing over (1, 2). A mature SC consists of two parallel structures, a pair of lateral elements that run along the entire length of the paired chromosomes and a centrally located structure (the central element), which are interconnected by transverse filaments (1, 2). Although the ultrastructure of the SC is evolutionarily conserved, the protein components share a very low level of amino acid sequence homology (2-4).

Genetic screens in *S. cerevisiae* have identified several mutants that exhibit defects in SC formation, leading to a decrease in the frequency of meiotic recombination, spore viability and improper chromosome segregation (5). Thus, ten meiosis-specific proteins, namely Hop1, Red1, Mek1, Hop2, Pch2, Zip1, Zip2, Zip3, Zip4, and Rec8, have been recognized as the bona fide components of the SC and/or are associated with the regulation of SC function (1, 2, 5-14). Briefly, their meiotic and cytological phenotypes are as follows: Zip1, which is present along the synapsed chromosomes, is an integral constituent of the central element. The *zip1* mutants have a defective SC, but they do not affect the pairing of homologous chromosomes (9). Zip2 and Zip3 co-localize at sites of synapsis initiation. Hence, the resulting Zip2/Zip3 complex is designated as the synapsis initiation complex (15-17). Pch2 is a pachytene checkpoint protein whose function is to inhibit intersister repair and promote interhomolog repair (18). Further, Pch2 is an AAA+ family ATPase that negatively regulates the function of Hop1 during normal meiosis; however, it exerts a positive action on the Hop1 protein (henceforth referred to as Hop1) under checkpoint inducing conditions (19, 20). Hop2, one of the SC-associated proteins represses the synapsis between non-homologous chromosomes (21, 22). Hop2 forms a complex with Mnd1 (Hop2-Mnd1 complex) that fosters homolog pairing (23-26). Mek1, a serine/threonine protein kinase, specifically promotes recombination between homologous chromosomes by preventing sister chromatid repair through its interaction with Hop1 and repair factor Rad54 (27-30).

S. cerevisiae Hop1, a structural component of the axial/lateral elements of SC, contains a Cys2/Cys2 zinc finger motif that is essential for its function (7, 8, 31). Previous studies have shown that Hop1 is a structure-selective DNA-binding protein, which exhibits high affinity for G-quadruplex structures and possesses the ability to form G4 DNA from an unfolded G-rich oligonucleotide (31, 32). The direct involvement of Hop1 in homolog pairing was suggested based on its ability to promote pairing of duplex DNA helices containing a centrally positioned G/C-rich region (33, 34). Further studies have revealed that Hop1 and its zinc finger motif show high affinity for the Holliday junction; they unwind the junction and thus imply a role in branch migration (35, 36). Strikingly, Hop1 can promote intra- and inter-molecular pairing between duplex

DNA molecules (37). Although the C-terminal fragment of Hop1 (Hop1 CTD) displayed all the known biochemical characteristics of full-length Hop1 *in vitro*, it failed to complement the meiotic recombination defects in *Δhop1* cells (38).

The *S. cerevisiae* Red1 protein (henceforth referred to as Red1), also a structural component of the axial/lateral element, was identified in a screen of meiotic lethal mutants (6). The *red1* mutants show chromosome missegregation, spore inviability and complete absence of SC formation (6, 39). Genome-wide chromatin immunoprecipitation studies have revealed that Red1 localizes to the meiotic pachytene chromosomes at the GC-rich regions (R-bands) in the genome, which are considered to be the hotspots of meiotic recombination (40-42). Bioinformatics analyses indicate that Red1 lacks sequence homology to any of the known proteins in the database (43). Further, Red1 physically interacts with subunits of the Rad 9-1-1 complex (28, 44, 45), indicating that Red1 functions as a downstream regulator of the meiotic DNA damage surveillance pathway that links the meiotic checkpoint to SC formation (45). The *hop1* and *red1* mutants display similar phenotypes and are placed under one epistasis group (39). An overexpression of *RED1* can suppress certain non-null *hop1* phenotypes (11). Additionally, Hop1 and Red1 interact with each other - physically and functionally (12, 39, 43, 46), and bind to SUMO chains prior to the initiation of meiotic interhomolog recombination and chromosome synapsis (47, 48). Although these studies suggest the importance of Red1 in meiosis, very little is known about the biochemical properties of Red1.

Here, we report overexpression and purification of the *S. cerevisiae RED1* gene product. In experiments with purified Red1, we found that it associates preferentially with the Holliday junction and other recombination/repair intermediates but not with single- or duplex DNA having single-stranded overhangs. It was also observed that Red1 possesses DNA end joining activity, thus implicating an unexpected and novel role for Red1 in recombination-based DNA repair. Moreover, Hop1 greatly stimulates the DNA end-joining activity of Red1. However, in contrast to Hop1, Red1, by itself, lacks the ability to promote intermolecular pairing between duplex DNA molecules but potentiates the pairing promoted by Hop1. These results are consistent with the idea that Red1 binding protects DNA structures that are obligatory meiotic recombination intermediates, and its DNA end joining activity contributes to the maintenance of genome integrity during meiotic chromosome synapsis and recombination.

RESULTS

Overexpression and purification of the full-length S. cerevisiae Red1 protein - Full-length untagged *S. cerevisiae* Red1 was expressed in and purified from *Escherichia coli* BL21 (DE3) CodonPlus-RIL cells. An analysis of whole cell lysates from uninduced and induced cell cultures by sodium dodecyl sulfate-polyacrylamide gel electrophoresis (SDS-PAGE) followed by Coomassie blue staining showed the presence of Red1 of 95.5 kDa in the pellet and soluble fraction (Fig.1A). The band corresponding to 95.5 kDa was undetectable in the whole cell lysates of cells grown in the absence of isopropyl β-D-1-thiogalactopyranoside (IPTG). Using

conventional chromatographic methods, untagged Red1 protein was purified to apparent homogeneity (Fig.1B, lane 5). In addition to the 95.5 kDa band, a proteolytic breakdown product of Red1 with a lower molecular weight was seen on an SDS-PAGE gel. This premise was corroborated by Western blot analysis using anti-Red1 antibodies (Fig.1B). The amount of full-length untagged Red1 in the protein preparation(s) used for the elucidation of its functional activities, which are described below, was >90%.

Affinity and kinetic measurements of the Red1 and Hop1 interaction - Genetic, co-immunoprecipitation and co-localization studies have demonstrated the physical interaction between Red1 and Hop1 proteins (12, 43, 46). A systematic mutant screen has identified a mutation in *RED1* (*red1-K348E*) that inhibited its interaction with Hop1, but it did not affect its homo-oligomerization (49). The yeast-two hybrid assay with *lexA-RED1* and *GAD-RED1*$^{537-827}$ variant forms exhibited a strong positive signal, indicating that the Red1 homo-oligomerization is mediated via its C-terminal region (12, 49). However, the affinity and kinetics of their interaction has not been investigated.

To confirm that the purified untagged protein was Red1, its ability to participate in protein-protein interactions with Hop1 was tested. For this purpose, two independent assays were used: far Western blotting and surface plasmon resonance (SPR). The interaction of Red1 with Hop1 was determined by a far Western blot assay using Red1 as a probe. The *S. cerevisiae* DNA damage checkpoint control protein Rad17 was used as a negative control. Red1 was observed to specifically interact with Hop1 in the assay, while Rad17 failed to do so (Fig. 2A). For an equilibrium analysis of affinity, increasing amounts of Red1 were added over immobilized Hop1 on a BIAcore CM5 sensor chip surface. The SPR response increased with increasing analyte concentration and reached equilibrium rapidly, reflecting fast kinetics. The representative sensorgrams are shown in Fig. 2B. The SPR response data was corrected for bulk refractive index effects and fitted using a 1:1 Langmuir binding model (A + B ↔ AB). An analysis of the affinity and kinetic parameters indicated that Red1 binds quantitatively to Hop1 with higher on-rate (2.44 X 10^4 $M^{-1}s^{-1}$) and slower off-rate (5.06 X 10^{-3} s^{-1}). The apparent dissociation constant (K_d) value derived from this data for the binding of Red1 to Hop1 was ~0.18 μM. These findings support the conclusion that the purified Red1 can interact *in vitro* with Hop1 and could also have biological activities.

Red1 exhibits high affinity for DNA recombination intermediates - Previous studies have revealed preferred DNA-binding sites for Red1 along the meiotic chromosomes (41, 42). For instance, the frequency and distribution analysis of Red1 foci in DNase I digested chromosome spreads, after immunostaining with anti-Red1 antibodies and antibodies to histone 2B, has revealed a tight association of Red1, but not histone 2B, along the axes of both homologs (42). Another study has shown that Red1 localizes preferentially to the DSB-active domains along chromosome III (41). In addition to being a component of the lateral element, Red1 also serves as a downstream signalling factor in the DNA damage surveillance pathway during meiosis (45). Furthermore, Red1 associates with Ddc1 and Mec3, which are the subunits of the 9-1-1 complex involved in meiotic DNA damage surveillance (45).

On the basis of these findings, it was hypothesized that Red1 can function directly via its interaction with genomic DNA sequences.

To gain an insight into the mechanistic aspects of Red1 function, a set of experiments were carried out to determine whether it has the ability to bind a variety of DNA substrates that are believed to be post-DSB recombination intermediates (Supplemental Table S1). Six different substrates were designed by annealing combinations of synthetic oligonucleotides (ODNs) (Supplemental Table S2). The DNA substrates included a branch immobile Holliday junction (HJ) containing four 20 bp arms, three-way junction with three 20 bp arms, flap structure containing 40 bp duplex DNA with a 20 nucleotide 5' flap single-strand, 40 bp blunt-ended duplex DNA, Y-shaped junction containing a 20 bp duplex region (dsDNA) with two 20 nucleotide heterologous single-strands and 20 bp DNA duplex with a 20 nucleotide 3' single-strand overhang and single-stranded DNA (ssDNA). The electrophoretic mobility shift assays were performed by incubating a constant amount (0.5 nM) of the specified ^{32}P-labeled substrate with increasing concentrations of Red1 ranging from 50 to 500 nM. The products of binding reactions were resolved by 6% PAGE under non-denaturing conditions and visualized as described in the Experimental Procedures section. It was found that Red1 showed significant differences in the relative binding affinity for different DNA substrates. Red1 preferentially bound to branched DNA structures, namely, the HJ and 3-way junction over the other substrates tested; the extent of its association increased with the addition of increasing Red1 concentrations (Fig. 3, A and B). In the assays performed with 5' flap, splayed DNA and blunt-ended duplex DNA, a similar pattern of interaction was noticed but the binding was relatively weak (Fig. 3, C to E). In sharp contrast to the binding with HJ and blunt- ended DNA duplex, very little or no binding was seen with ssDNA or partial DNA duplex containing a 3' overhang (Fig. 3, F and G).

To ascertain the DNA binding preferences, the amount of DNA bound was quantified and plotted against a range of input concentrations of Red1. It was found that the Red1 binding exhibits a hyperbolic dependence on its concentration and a hierarchial substrate preference (Fig. 3H). Specifically, Red1 shows a higher binding affinity towards HJ, followed by replication fork (RF) > 5' flap > Y-shaped structure > duplex DNA > dsDNA with a 3' overhang> ssDNA. These results support a model in which ssDNA or ssDNA tethered to a duplex is not energetically favorable to the DNA binding activity of Red1. Next, the equilibrium dissociation constants for the interaction of Red1 with different DNA substrates were derived. The relative DNA affinity of Red1 was estimated from slopes of linear regression curves fitted to the data points. As seen in Table 1, the affinity of Red1 to the HJ is significantly greater yielding an apparent K_d value of 66 nM, which is two-fold lower than the value obtained for the 3-way junction. In contrast, Red1 exhibited very weak affinity for the Y-shaped DNA duplex while exhibiting measurable but insignificant binding to the duplex with a 3' overhang or ssDNA. This approach can differentiate the DNA binding specificities; nevertheless the K_d values should be interpreted cautiously because electrophoretic mobility shift assay (EMSA) is a quasi-equilibrium assay and the presence of other proteins could modify the substrate specificity of Red1 *in vivo*. However, the data provide compelling evidence that Red1 binds directly to DNA

and possesses structure-selective DNA binding activities.

Red1 forms highly stable complexes with the HJ and 3-way junction - To further characterize the specificity of Red1-DNA interactions, the effect of ionic strength on the stability of pre-formed Red1 nucleoprotein complexes was tested. The assays were set up with a fixed amount of Red1 that was sufficient to bind all the DNA present in the reaction mixtures (Fig. 4, lane 2). The reactions were quenched and the products were resolved on EMSA gels. As shown in Fig. 4, marked differences were observed in the stability of complexes formed by Red1 with various substrates. In good agreement with the data presented in Fig. 3, Red1 formed highly stable complexes with the HJ and 3-way junction and they were not affected even by the presence of 500 mM NaCl. However, the stability of complexes formed with blunt-ended dsDNA was affected by changes in the ionic strength. To determine quantitative changes, the amount of free and bound DNA in each lane was quantified and the data is expressed relative to salt concentration. It was found that ~80% of the complexes formed with blunt-ended dsDNA dissociated in the presence of 1 M NaCl, in contrast to a modest dissociation (~20%) of protein-DNA complexes formed with either the HJ or RF at the same concentration (Fig. 4D). The progressive retardation of free-DNA (Fig. 4C) could be due to the corresponding increase of salt in the reaction mixture. These results support the idea that Red1 forms thermodynamically stable complexes with the HJ and RF than with the blunt-ended dsDNA and that hydrophobic interactions also contribute to the stability of the complex.

Red1 potentiates Hop1 promoted pairing of DNA double helices containing G/C-rich regions - The mechanisms underlying the processes of homology search and synapsis of homologous chromosomes are not fully understood (1, 2, 4). It has been hypothesized that G4 DNA forming regions along the entire length of a chromosome may be used to bring together the four chromatids to establish synapsis during meiosis (50-54). Our previous work has shown that Hop1 promotes intra- and inter-molecular pairing of double-stranded DNA molecules (33, 34, 37). The pairing was further augmented by a centrally positioned G/C-rich region (33, 34). In light of these studies, we asked whether Red1, by itself, can promote intermolecular pairing between two DNA duplex molecules. To verify this, an *in vitro* assay using a 48 bp synthetic duplex DNA with a single centrally positioned 8 bp G/C sequence was employed (33, 34). First, the ability of Red1 to bind to the 48 bp DNA duplex containing a centrally positioned 8 bp G/C sequence was tested in comparison to a mixed-sequence DNA duplex of identical length (Fig. 5, A and B). The assay was performed with a constant amount (2 nM) of DNA duplex and increasing concentrations of Red1 ranging from 0-2 μM. The reaction products were resolved on nondenaturing polyacrylamide gels. As shown in Fig. 5, C and E, incubation with Red1 shifted the free DNA to a slowly migrating protein-DNA complex, which increased with increasing Red1 concentration. However, the relative binding efficiency of Red1 for mixed-sequence DNA duplex was higher compared to the DNA duplex containing the G/C region. To determine if Red1 promotes pairing between two DNA duplex molecules, experiments were conducted in parallel. In these tests, the reaction mixtures were deproteinized by proteinase

K and SDS and the products were separated on 10% nondenaturing polyacrylamide gels. In both cases, no evidence was found to support a role for Red1 in the pairing of two duplex DNA molecules (Fig. 5, D and F).

Previous studies have shown genetic and physical interaction between Red1 and Hop1. The overexpression of *HOP1* suppresses certain *red1* alleles, and vice versa (12, 42, 46). In line with these findings, we asked whether Red1 can modulate the DNA pairing activity of Hop1. We performed EMSA with the same ^{32}P-labeled DNA duplex containing a centrally-embedded 8 bp G/C region. In one experiment, a constant amount of DNA duplex was incubated with increasing concentrations of Hop1. In a second experiment, the same reaction was performed with a constant amount of Hop1 in the presence of increasing concentrations of Red1. The reaction mixtures were deproteinized and the products were analyzed as described above. It was found that Hop1 can promote intermolecular pairing between two duplex DNA molecules that are highly reminiscent of those seen before (33, 34) (Fig. 6B). Importantly, however, the findings of the second experiment pointed out that the DNA pairing activity of Hop1 is potentiated by Red1 in a concentration-dependent manner (Fig. 6C). Further, quantitative analysis of the product formed with a phosphorimager revealed that Red1 is able to stimulate the DNA pairing activity of Hop1 by two-fold (Fig. 6D).

We next investigated the effect of sequence-specific and non-specific competitor DNAs on the pairing activity. The assay was performed as described above, except that the unlabeled competitor DNA duplex was added in various concentrations. The reaction products were resolved on non-denaturing polyacrylamide gels. Fig. 7, A and B, show gel images illustrating significant qualitative differences in the pattern of inhibition by specific (DNA duplex containing a single centrally-embedded 8 bp G/C region) and non-specific (mixed-sequence DNA duplex) DNAs on the pairing activity of Hop1 and Red1. The addition of a specific competitor strongly decreased product formation in a concentration-dependent manner compared to a non-specific competitor; in both cases, no intermediate species were generated. In fact, differences in the pattern of suppression between specific and non-specific DNAs were evident at all the concentrations that were examined. A quantitative analysis of the amount of product formed revealed that the suppression of DNA pairing was more pronounced in the presence of specific-sequence compared to non-specific DNA (Fig. 7C). The difference is most obvious at a 100-fold molar excess of each of the competitors; here, the specific competitor DNA suppressed product formation to >95% whereas the non-specific competitor suppressed it to 5%.

Red1 promotes intramolecular bridging of non-contiguous segments in a circular duplex DNA - To gain further insights into the DNA binding mode of Red1, atomic force microscopy (AFM) was used to reveal the architecture of Red1-DNA complexes. Following a published protocol (37, 38), the binding of Red1 to pUC19 circular duplex DNA was first examined using the conditions developed for its binding to DNA. After incubation, 5 µl aliquots were placed on freshly cleaved mica; they were allowed 2 min for absorption, and then visualized using tapping-mode AFM. At low concentrations of Red1, plasmid DNA associated with Red1 were observed at various positions,

leading to intramolecular bridging between non-contiguous segments of DNA [Fig. 8A, panels (ii) to (iv). Although a similar pattern of binding was observed at higher concentrations of Red1, the nucleoprotein filament frequency and length increased at this concentration [Fig. 8B, panels (i) to (v). Quantification of the frequency of various types of Red1-bound DNA structures revealed at least four different types of DNA binding events: (1) binding of Red1 at random positions; (2) Red1-bound intramolecular nodes; (3) intramolecular stem-loop structures and (4) Red1 nucleoprotein filaments. The contour length of the Red1-DNA complexes gradually decreased ~3-fold concomitant with the increase in Red1 concentration, pointing out that Red1 induces DNA compaction. Interestingly, in contrast to Hop1 (37), no intermolecular alignment of circular plasmid DNA molecules was detected in the presence of Red1 under these conditions. A number of AFM images were subjected to statistical analysis to quantify the Red1-DNA complexes. The analysis revealed that >80% of the plasmid DNA molecules are associated with Red1 to generate various structures (Fig. 8C-D).

Red1 promotes non-homologous DNA end joining - These foregoing results prompted us to further explore (using AFM) the mode of binding of Red1 to linear plasmid DNA. To this end, the pUC19 linear duplex DNA at two concentration of Red1 was incubated and the protein-DNA complexes were visualized as described above. The results were striking: the formation of concatemeric DNA was observed: this is due to the end-to-end joining of unit lengths of linear plasmid DNA (Fig. 9A-B) It was also noticed that Red1 localizes mostly at the ends and interface between two linear DNA duplex molecules, in addition to being bound at many different sites on the DNA molecule. However, in contrast to Hop1 (37), crossover structures resulting from the intermolecular alignment of two linear duplex DNA molecules were not observed in the presence of Red1. Nonetheless, these results are consistent with the idea that Red1 binding may lead to higher-order assembly of DNA through the end joining of linear duplex DNA helices. Further, a quantification analysis suggested that the linear multimerization promoted by Red1 increases in a concentration-dependent manner (Fig. 9C). Despite the different nature of the assays, the AFM evidence that Red1 was unable to promote the pairing of DNA molecules is in good agreement with data from the gel assays (Fig. 6).

Hop1 stimulates the intermolecular ligation of linear dsDNA molecules promoted by Red1 – In light of the fact that Red1 and Hop1 proteins physically interact with each other (12, 39, 43, 46), we tested the effect of Hop1 on non-homologous DNA end-joining activity or Red1. The assay was carried out by incubating blunt-ended linear dsDNA with Red1 in the presence of various concentrations of Hop1. The DNA products of this reaction were separated by agarose gel electrophoresis (see “Experimental Procedures”). Whereas Red1 alone displayed significant amount of DNA end-joining activity (Fig. 10, lane 5), Hop1 greatly potentiated the ligation of linear dsDNA molecules to form dimers, trimers, etc (Fig. 10, lanes 6-9). The products were found to be sensitive to exonuclease III treatment, thus confirming the formation of linear multimers of the blunt-ended 2.6-kb plasmid DNA substrate (Fig.10, lanes 10-12). We note that Hop1 by itself promotes bridging between linear dsDNA molecules to form mulitimers (37), which is not apparent at the concentration

tested here (Fig. 10, lane 4). Therefore, the question whether Hop1 can stimulate Red1 promoted DNA end-joining activity needs further study. Collectively, these *in vitro* results support the genetic evidence and further underscore the importance of physical interaction between Hop1 and Red1.

DISCUSSION

Despite significant progress in defining the protein components of *S. cerevisiae* SC and their localization to specific substructures of the tripartite complex, the function of these different proteins is not fully understood. Towards this goal, a biochemical approach was adopted to elucidate the mode of action of Red1. In this study, we provide the first direct evidence that Red1 is a sequence non-specific but structure-selective DNA binding protein, associates preferentially with DNA substrates that are considered as obligatory meiotic recombination intermediates, promotes DNA bridging and non-homologous DNA end-joining as well as potentiates Hop1 promoted pairing of dsDNA molecules. Moreover, Hop1 greatly stimulates the DNA end-joining activity of Red1.

Previous genetic and biochemical studies on *S. cerevisiae* have established the molecular mechanism(s) of homologous recombination (HR) in meiosis. Briefly, HR between paired homologous chromosomes begins with the incision of a DSB at the recombination hotspot by a topoisomerase-like protein, Spo11 (55, 56). Following the generation of 3' single-stranded tails on either side of the break by the coordinated action of helicase/nuclease activities encoded by *MRE11/XRS2/RAD50*/*SAE2* genes, the Rad51 and Dmc1 proteins polymerize on ssDNA thus generated to form a helical filament (1, 2, 4). The resulting nucleoprotein filament invades homologous dsDNA to produce D-loops. Subsequently, the D-loops are extended by repair synthesis to form heteroduplex DNA. A number of accessory factors either facilitate the activity of Rad51/Dmc1 or promote strand transfer by themselves. The strand exchange yields a 3-way junction, When the heteroduplex DNA encounters the ssDNA-dsDNA junction on the invading strand, the 3-stranded joint molecule is converted into a 4-stranded Holliday junction. Multiple pathways exist in eukaryotic cells for processing and resolution of the HJ (57). In somatic cells, four proteins comprising BLM, topoisomerase IIIa, RMI1, and RMI2, termed as the BTR complex [in *S. cerevisiae*, orthologs of the BTR complex are Sgs1-Top3-Rmi1 (STR complex)], promote the convergent migration of two HJs to produce a hemicatenane that can be processed by topoisomerase action. In *S. cerevisiae sgs1* mutants, the joint molecules are processed by Mus81-Mms4 (the ortholog of *MUS81-EME1*) and Yen1 (the ortholog of *GEN1*), generating both crossover and non-crossover products (58-61).The second and third pathways utilize structure-selective endonucleases that cleave the HJs to generate crossover and non-crossover products (57).

The understanding of the mechanisms of homologous DNA pairing, strand exchange and HJ resolution in eukaryotes has advanced considerably since the isolation of Rad51 and Dmc1 proteins (62, 63). However, knowledge of the functions of SC components is scanty. Genetic studies have shown that *red1* and *hop1* mutations perturb the same subset of events during meiotic recombination (39). Accordingly, an overexpression of *RED1* suppresses or escalates certain non-null

hop1 alleles (11, 64). The mutation of *RED1* in a *DMC1* diploid cells leads to the disappearance of DSBs, thereby giving rise to the display of meiotic division abnormalities and non-viable spores (65-67). These genetic findings are most consistent with our observations that Red1 possesses DSB-binding and DNA end joining activities. Further, *red1* mutants are pleiotropic; consequently, they show a number of mutant phenotypes including unusual defects in chromosome structure and synapsis (39, 67). Genetic data from *S. cerevisiae* indicate that mutations in *hop1, red1, and mek1* specifically reduce interhomolog recombination and generate inviable spores, indicating that *HOP1* acts as a barrier to sister chromatid repair (68). Besides Hop1, Red1 also interacts with Mek1 and subunits of the 9-1-1 checkpoint module (Rad17-Mec1-Ddc1) through the Ddc1-Mec3 subunit-specific motifs (45, 69). Consistent with the genetic data, immunoprecipitation experiments have shown that Red1/Hop1 and Red1/Mek1 form complexes in meiotic cells (46, 69, 70, 71). While the role of Red1 in acting as a barrier to sister chromatid repair in meiotic cells has been appreciated for over 20 years, the exact mechanism of *RED1* function in establishing interhomolog bias has not been elucidated. To interpret the genetic results, it is important to determine the biochemical properties of Red1 and its functional relationship to Hop1.

Several experiments in the current investigation demonstrate that purified Red1 associates preferentially with the duplex DNA and 3-way junction as well as the Holliday junction compared to ssDNA and dsDNA with single-stranded overhangs. Furthermore, the broad substrate specificity of Red1 indicates that it can engage in a wide range of DNA binding events, induce condensation and topological changes. It also suggests that these functional outcomes may vary according to the specific substrate and the availability of interacting partners. The finding of the present study that Red1 induces DNA bridging, condensation and formation of stem-loop structures implies a strong probability of its involvement in the folding of prophase I chromosomes into radial loops; this, in turn, may facilitate tethering of the loops to the SC axial/lateral elements (72). Nevertheless, what does it mean for Red1, a lateral element protein of SC formed during early meiosis, to have a high affinity for a late DNA recombination intermediate such as the HJ? Although Red1 is thought to be a crucial regulator of early meiosis, it physically associates with the ring-shaped 9-1-1 complex, a downstream effector essential for the meiotic DNA damage surveillance pathway (45). Association of 9-1-1 with Red1 is required for meiotic checkpoint activation (45, 69), and Red1 by itself binds to DSBs and promotes DNA end joining (this study), but its function at different phases of meiotic prophase I remains unclear. Given these findings, we propose that Red1 also functions at mid- and late pachytene phases by monitoring the DNA integrity and progression of meiotic recombination intermediates, including the DSBs and Holliday junction.

Previous studies have implicated Red1 in several aspects of meiotic recombination (5, 6, 39, 65). Evidently, R/G-band regions modulate the frequency HR: Red1 promotes the formation of DSBs at both R- and G-bands and then assists the loading of Dmc1 on ssDNA, specifically by counteracting the adverse effects of R-bands (41). Significant insights into the role of G-quadruplexes in meiosis emerged from genetic studies in *S. cerevisiae*: deletion of *KEM1/SEP1*, which encodes a G-quadruplex DNA specific nuclease, arrests the cells at meiotic

prophase I (73). Genome-wide studies on *S. cerevisiae* have revealed the existence of more than 1500 sequence motifs with the potential to form G-quadruplex structures; these motifs overlap with the meiotic DSBs (74, 75). Additionally, a strong correlation has been established between meiotic DSBs, recombination rate and G/C content in *S. cerevisiae* (76, 77). The occurrence of high concentrations of potential G-quadruplex forming sequences in the *S. cerevisiae* genome strongly implicates a role for these sequences in meiotic recombination (78, 79). Furthermore, the MRX complex, composed of Mre11, Rad50 and Xrs2, which is involved in the resection of DSBs, has a high affinity for G4 structures *in vitro* (80, 81). There is good evidence that intragenomic DNA recombination in the *pilE* locus is controlled by the G-quadruplex DNA (82). Altogether, these findings highlight an important role for the G-quadruplex DNA based mechanism that it might be involved in chromosome pairing and recombination.

Although both Hop1 and Red1 associate independently with chromosomes at the leptotene stage to form a series of foci, the association of Hop1 is dependent on Red1 (42). Several studies have demonstrated that the incision of programmed meiotic DSBs and the loading of Red1 coincide with GC-rich regions (40, 41, 76). Intriguingly, we found that Red1 and Hop1 proteins exhibit similar affinities for dsDNA containing the G/C region *in vitro*, but the functional consequences of the two proteins appear to be different at least in one important way: Red1 lacks the ability to promote the pairing of two linear dsDNA molecules. However, these results do not exclude the possibility that Red1 contains low levels of DNA pairing activity that is not apparent under these conditions. In addition, the failure of Red1 to promote pairing between duplex molecules is not due to its inability to bind G-quadruplex DNA because it binds to G4 DNA at nearly the same affinity as does Hop1 (data not shown). On the other hand, the positive interaction between Hop1 and Red1 in potentiating the pairing of two DNA molecules and DNA end-joining probably provides a huge advantage in terms of selectivity and specificity during meiosis.

The formation of synapsis product promoted by Hop1 or Hop1 plus Red1 does not reach 100% equilibrium. Although we do not know the precise reason(s), one plausible explanation is that Hop1/Red1 protein(s) also promote pairing of duplex DNA molecules at regions of “low G/C-content.” Upon deproteinization of the reaction mixtures, the synapsis product(s) formed at low G/C content perish resulting in 30-40% product formation. Recently, two independent studies conducted in mouse and *S. cerevisiae* have discovered a key role for a chromosomally tethered proteasome in the regulation of chromosome synapsis and recombination during prophase of meiosis I (83, 84). This hints that inappropriate synapsis and protein degradation are important for the interrelated molecular pathways that execute synapsis and recombination of meiotic chromosomes.

What are the consequences of the direct interaction between Red1 and Hop1? While Hop1 and Red1 can independently bind various meiotic recombination intermediates, Red1 and Hop1 unite to perform an important function: potentiate the pairing of two dsDNA molecules. The results reveal that Hop1 acts earlier than Red1, at least in DNA pairing events. In agreement with these results genetic evidence has shown the existence of Hop1/Red1 hetero-oligomers (11, 12, 85). Thus, the functional

interaction between Hop1 and Red1 in the pairing of dsDNA molecules is a functional validation of their genetic/physical interaction. Notwithstanding, what specialized function can Red1 perform in the cell if it acts independently? We assume that DNA end joining, DNA bridging and looping activities of Red1 fit well with the condensation of chromosomes during the meiotic prophase I. In summary, this study, for the first time, has revealed a biochemical function for Red1. In particular our results highlight a crucial role for Red1 during prophase of meiotic division I. In addition to its structural role in the SC, Red1 potentiates pairing of DNA molecules by Hop1, and also promotes the joining of broken DNA ends, which, in turn, might protect meiotic recombination intermediates and prevent the loss of genetic material. The fact that Hop1 and Red1 act independently of each other, and also together, could allow them to perform different functions at separate steps during chromosome synapsis and recombination.

EXPERIMENTAL PROCEDURES

Source of biochemicals, bacterial strains, proteins and DNA oligonucleotides - Fine chemicals were purchased from GE Biosciences and Sigma, USA. Restriction endonucleases, T4 DNA ligase and T4 polynucleotide kinase were purchased from New England Biolabs and Thermo Scientific. All the reagents used were of analytical grade. The DNA oligonucleotides were synthesized by Sigma-Genosys. [γ-^{32}P] ATP was purchased from Bhabha Atomic Research Centre, Mumbai, India. *Escherichia coli* expression strain RIL and the expression vectors pET-22b and pET-28a were purchased from Novagen (USA). Protein purification resins Ni^{2+}-NTA agarose, SP Sepharose and Q Sepharose were purchased from Qiagen and Sigma, USA. Fast performance liquid chromatography columns were purchased from GE Biosciences. The Red1 antibodies were custom-made against Red1 protein in rabbits by Imgenex India, Bhubaneswar, India. The full-length Hop1 was purified as previously described (86).

Molecular cloning of the S. cerevisiae RED1 gene - The nucleotide sequence corresponding to *S. cerevisiae RED1* (2484 bp) was PCR amplified from the plasmid plb-1 (11) using specific primers (Supplemental Table S2). The PCR product was purified from the agarose gel using Qiagen's gel extraction kit. The product was digested by NdeI and HindIII and directionally cloned into expression pET-22b vector (Novagen). The resulting recombinant plasmid was designated *pRED1*.

Overexpression and purification of the Red1 protein - *S. cerevisiae* Red1 was expressed and purified from *E. coli* BL21 (DE3) CodonPlus-RIL cells, which were transformed with the p*RED1* plasmid. A single colony from a freshly grown transformation plate was inoculated into 30 ml of LB broth supplemented with 100 µg/ml ampicillin and was grown overnight at 37 ^{o}C. This overnight culture was then inoculated into 2 L of LB broth supplemented with 100 µg/ml of ampicillin. The cells were grown at 37 ^{o}C with vigorous shaking. The expression of Red1 was induced by the addition of 0.5 mM IPTG after the culture reached an OD of 0.5 at 600 nm; the incubation was extended for 12 h. The cells were collected by centrifugation, washed with STE buffer [10 mM Tris-HCl (pH 8), 100 mM NaCl and 1 mM EDTA] and resuspended in buffer A [20 mM Tris-HCl (pH 8), 10% glycerol, 50

mM NaCl and 5 mM 2-mercaptoethanol] and stored at -80 ^{o}C. These cells were thawed and lysed by sonication (Model No. GEX-750, Ultrasonic Processor) on ice at 51% duty cycles in a pulse mode. The sonicated suspension was centrifuged in a Beckman type 45 Ti rotor at 30000 rpm for 1 h at 4 ^{o}C. The supernatant was subjected to $(NH_4)_2SO_4$ precipitation at 55% saturation followed by centrifugation at 18000 rpm at 4 ^{o}C for 30 min. The pellet was resuspended in buffer A and dialysed against the same buffer. The dialysate was chromatographed on a Q Sepharose column equilibrated with buffer A. The Red1 protein was eluted from the column in the flow-through fractions. The flow-through was subjected to $(NH_4)_2SO_4$ precipitation at 50% saturation. The precipitated protein was collected by centrifugation at 18000 rpm for 30 min at 4 ^{o}C. The pellet was resuspended in buffer B [20 mM HEPES-HCl (pH 8), 1 M NaCl, 10% glycerol and 5 mM 2-mercaptoethanol] and dialysed against the same buffer. The dialysate was passed through a Sephadex 200 (S-200) gel filtration column equilibrated with buffer B, and eluted using buffer B. The fractions containing Red1 were pooled and dialysed against buffer C [20 mM HEPES-HCl (pH 8), 250 mM NaCl, 50% glycerol and 1 mM DTT]. The purity of Red1 was assessed by SDS-PAGE, followed by Coomassie blue staining. Aliquots of the Red1 protein were stored at -80 ^{o}C. The concentration of Red1 was determined by the dye-binding method using the bovine serum albumin as a standard (87).

Far Western blotting assay - Increasing concentrations of purified Hop1 or Rad17 (1 to 5 µg) diluted in buffer A [10 mM HEPES-HCl (pH 7.5), 100 mM NaCl (pH 7.5) and 1 mM EDTA] were spotted onto a nitrocellulose membranes. Thereafter, blocking was carried out at 4 ^{o}C for 4 h with buffer A containing 5% (w/v) nonfat milk and then incubated with Red1 for 9 h at 4 °C. The membranes were washed once with buffer A prior to incubation with anti-Red1 antibody for 12 h at 4 ^{o}C. The membranes were washed six times for 10 min with PBS containing 0.1 % Tween-20 (PBST) and incubated with a 1:40000 dilution of horseradish peroxidase-conjugated anti-rabbit antibody for 2 h at 4 ^{o}C. Finally, the membranes were washed three times with PBST and the antibody signals were visualized using a chemiluminescence imaging device.

Preparation of DNA substrates - The ODNs used for construction of the DNA substrates are listed in Supplemental Table S2. The ODNs were labeled at the 5' end using [γ-^{32}P]ATP and T4 polynucleotide kinase (88). The DNA substrates were constructed using different combinations of ODNs (Supplemental Table S1). Briefly, stoichiometric amounts of the purified ODNs were annealed by incubation in 0.3 M sodium citrate buffer (pH 7) in a 100 µl reaction mixture containing 3 M NaCl at 95 ^{o}C followed by slow cooling to 4 ^{o}C over a period of 2 h. The Holliday junction, Y-shaped substrates, and other intermediates of DNA replication/repair were prepared and characterized as described (89). In the case of substrates used for the DNA pairing assay, the top strand of the duplex DNA was labeled at the 5' end using [γ-^{32}P]ATP and T4 polynucleotide kinase. The labeled strand was annealed to an equimolar amount of unlabeled complementary strand. To purify the substrates, the reaction mixtures were subjected to electrophoresis on 8% (w/v) polyacrylamide gel in 45 mM Tris–borate buffer (pH 8.3) containing 1 mM EDTA and 120 mM KCl at 10 V/cm for 5-12 h. The

bands corresponding to specific substrates were excised from the gel and eluted in TE buffer [10 mM Tris-HCl (pH 7.5), 1 mM EDTA].

Surface plasmon resonance measurements - All the measurements were performed with a Biacore 2000 optical biosensor (GE Healthcare Life Science). Protein immobilization, binding experiments, and data analysis were performed according to the manufacturer's protocol and software supplied with the instrument. Hop1 was immobilized on the surface of a CM5 sensor chip (~1000 response units/flow cell) using the amine coupling method. The unbound protein was removed by passing the buffer with a flow rate of 100 µl/min. The flow cell 1 was used as a control. The binding experiments were carried out at 30 °C using a continuous flow of the running buffer [10 mM HEPES buffer (pH 7.5) containing 150 mM NaCl, 50 mM EDTA and 0.005% P-20 surfactant] at a flow rate of 50 µl/min. Increasing concentrations of Red1 (40-320 nM) were added over the CM5 sensor chip. Regeneration was carried out by 4 M $MgCl_2$. The data obtained for the interaction of Red1 with Hop1 was corrected for nonspecific binding by the automatic subtraction of blank data from in-line reference flow cells. The data was analyzed using a 1:1 Langmuir binding model. A global fit of the data was used to determine the kinetic constants using the BIAcore evaluation software 3.0.

DNA binding assay - The reaction mixtures (20 µl) contained 10 mM HEPES-HCl (pH 7.5) or 10 mM Tris-HCl (pH 7.5), 0.5 nM of the specified ^{32}P-labeled DNA substrate and increasing concentrations of the specified protein. The mixtures were incubated at 30 ^{o}C for 30 min. The reaction was terminated by the addition of 2 µl loading dye (0.25% xylene cyanol, 0.25% bromo phenol blue in 20% glycerol). The reaction mixtures were electrophoresed on a 6% native polyacrylamide gel in 44.5 mM Tris–borate buffer (pH 8.3) containing 1 mM EDTA at 10 V/cm at 4 ^{o}C for 3-6 h. The gels were dried and exposed to phosphorimager screen (FLA-9000); the bands were visualized using the software supplied by the manufacturer. The data was quantified using the UVI band map software package and plotted in the Graph Prism software.

DNA pairing assay - The reaction mixtures (20 µl) contained 2 nM ^{32}P-labeled duplex DNA, 10 mM HEPES-HCl (pH 7.5) or 10 mM Tris-HC (pH 7.5) and increasing concentrations of the specified protein. After incubation at 30 ^{o}C for 30 min, the mixtures were deproteinized by the addition of proteinase K (0.2 mg/ml) and SDS (0.2%) followed by incubation at 37 ^{o}C for 20 min. The reactions were terminated by the addition of 2 µl loading dye (0.25% xylene cyanol, 0.25% bromo phenol blue in 20% glycerol). The reaction mixtures were electrophoresed on a 10% native polyacrylamide gel in 44.5 mM Tris–borate buffer (pH 8.3) containing 1 mM EDTA at 10 V/cm at 4 ^{o}C for 6 h. The gels were dried and visualized by the FLA-9000 phosphoimager. The data was quantified using using the UVI band map software package and plotted in the Graph Prism software.

AFM imaging of DNA and Red1-DNA complexes - The plasmid pUC19 was isolated from *E. coli* DH5α cultures and used for imaging the Red1-DNA complexes. The plasmid DNA was purified using the Thermo Scientific Maxi-prep kit and resuspended in water. Subsequently, the plasmid was treated with chloroform:

isoamyl alcohol to remove the intrinsically bound proteins. Blunt-ended linear pUC19 DNA was generated by digestion of circular pUC19 DNA with SmaI. Red1 (100 nM and 300 nM) was incubated with 5 ng of circular or linear pUC19 DNA in 10 µl of reaction mixture containing 20 mM Tris-HCl (pH 8) and 2 mM $MgCl_2$. After incubation at 30 ºC for 30 min, 5 µl of aliquot was applied to the surface of freshly cleaved mica. The mica surface was rapidly rinsed with nanopure deionized water and air dried. The images were acquired in tapping mode using an SNL (silicon tip on nitride lever) probe (Agilent Technologies, spring constant 21-98 N/M).

DNA ligation assay – One hundred ng of blunt-ended 2.6 kb pUC19 DNA (generated by digestion of circular pUC19 DNA with SmaI) was incubated in the absence or presence of specified concentrations of Red1 and Hop1 in a 20 µl reaction mixture containing 20 mM Tris-HCl (pH 8). After incubation at 30 °C for 30 min, 2 µl of T4 DNA ligase buffer and 10 units of T4 DNA ligase (Thermo Scientific) were added and the incubation was extended at 30 °C for 20 min. For reactions involving exonuclease III (Exo III), samples were further incubated at 37 °C for 30 min in the presence of 5 units of Exo III (New England Biolabs). The reactions were terminated by the addition of 1 µl of 20% SDS and 1 µl of 10 mg/ml proteinase K and incubated at 37 °C for 30 min. The samples were electrophoresed through 1.1% agarose in 45 mM Tris borate buffer (pH 8.3) containing 1 mM EDTA at 80 V for 7 h and visualized by staining with ethidium bromide.

Acknowledgements

We thank Krishnendu Khan for his help in *S. cerevisiae RED1* gene cloning and N. S. SriLatha for her assistance in SPR measurements.

Footnotes

This work was supported by a grant (SR/SO/BB-94/2010) from the Department of Science and Technology, New Delhi. K.M. is the recipient of the J. C. Bose National Fellowship (SR/S2/JCB-24/2005) from the Department of Science and Technology, New Delhi.

Conflict of interest: The authors declare that they have no conflicts of interest with the contents of this article.

Author contributions: KM conceived and designed the project and wrote the manuscript. RK performed experiments and contributed to the writing of the manuscript. IG performed the AFM measurements. KM, RK and IG analyzed the data and interpreted the results. All authors read and approved the final manuscript.

REFERENCES

1. Zickler, D., and Kleckner, N. (2015) Recombination, pairing, and synapsis of homologs during meiosis. *Cold Spring Harb. Perspect. Biol*. **7 (6)**, pii: a016626. doi: 10.1101/cshperspect.a016626
2. Cahoon, C. K., and Hawley, R. S. (2016) Regulating the construction and demolition of the synaptonemal complex*. Nat. Struct. Mol. Biol*. **23,** 369-377

3. Page, S. L., and Hawley, R. S. (2004) The genetics and molecular biology of the synaptonemal complex. *Annu. Rev. Cell Dev. Biol*. **20,** 525-558
4. Anuradha, S., and Muniyappa, K. (2005) Molecular aspects of meiotic chromosome synapsis and recombination. *Prog. Nucl. Acids Res. Mol. Biol.***79,** 49-132
5. Mao-Draayer, Y., Galbraith, A. M., Pittman, D. L., Cool, M., and Malone, R. E. (1996) Analysis of meiotic recombination pathways in the yeast *Saccharomyces cerevisiae. Genetics* **144**, 71-86
6. Rockmill, B., and Roeder, G. S. (1988) *RED1*: a yeast gene required for the segregation of chromosomes during the reductional division of meiosis. *Proc. Natl. Acad. Sci. U.S.A.* **85**, 6057-6061
7. Hollingsworth, N. M., and Byers, B. (1989) *HOP1:* a yeast meiotic pairing gene. *Genetics* **121**, 445-462
8. Hollingsworth, N. M., Goetsch, L., and Byers, B. (1990) The *HOP1* gene encodes a meiosis-specific component of yeast chromosomes. *Cell* **61**, 73-84
9. Sym, M., Engebrecht, J. A., and Roeder, G. S. (1993) *ZIP1* is a synaptonemal complex protein required for meiotic chromosome synapsis. *Cell* **72**, 365-378
10. Agarwal, S., and Roeder, G. S. (2000) Zip3 provides a link between recombination enzymes and synaptonemal complex proteins. *Cell* **102**, 245-255
11. Hollingsworth, N. M., and Johnson, A. D. (1993) A conditional allele of the *Saccharomyces cerevisiae HOP1* gene is suppressed by overexpression of two other meiosis-specific genes: *RED1* and *REC104*. *Genetics* **133**, 785-797
12. Hollingsworth, N. M., and Ponte, L. (1997) Genetic interactions between *HOP1, RED1* and *MEK1* suggest that *MEK1* regulates assembly of axial element components during meiosis in the yeast *Saccharomyces cerevisiae*. *Genetics* **147**, 33-42
13. Joshi, N., Brown, M. S., Bishop, D. K., and Borner, G. V. (2015) Gradual implementation of the meiotic recombination program via checkpoint pathways controlled by global DSB levels. *Mol. Cell* **57**, 797-811
14. Vader, G. (2015) Pch2(TRIP13): controlling cell division through regulation of HORMA domains. *Chromosoma* **124**, 333-339
15. Fung, J. C., Rockmill, B., Odell, M., and Roeder, G. S. (2004) Imposition of crossover interference through the nonrandom distribution of synapsis initiation complexes. *Cell* **116**, 795-802
16. Lynn, A., Soucek, R., and Borner, G. V. (2007) ZMM proteins during meiosis: crossover artists at work. *Chromosome Res*. **15**, 591-605
17. Macqueen, A. J., and Roeder, G. S. (2009) Fpr3 and Zip3 ensure that initiation of meiotic recombination precedes chromosome synapsis in budding yeast. Curr. Biol. **19**, 1519-1526
18. Zanders, S., Sonntag Brown, M., Chen, C., and Alani, E. (2011) Pch2 modulates chromatid partner choice during meiotic double-strand break repair in *Saccharomyces cerevisiae*. *Genetics* **188**, 511-521
19. Chen, C., Jomaa, A., Ortega, J., and Alani, E. E. (2014) Pch2 is a hexameric ring ATPase that remodels the chromosome axis protein Hop1. *Proc. Natl. Acad. Sci. U.S.A.* **111**, E44-53
20. Herruzo, E., Ontoso, D., Gonzalez-Arranz, S., Cavero, S., Lechuga, A., and San-Segundo, P. A. (2016) The Pch2 AAA+ ATPase promotes phosphorylation of the

Hop1 meiotic checkpoint adaptor in response to synaptonemal complex defects. *Nucl. Acids Res*. **44**, 7722-7741
21. Leu, J. Y., Chua, P. R., and Roeder, G. S. (1998) The meiosis-specific Hop2 protein of *S. cerevisiae* ensures synapsis between homologous chromosomes. *Cell* **94**, 375-386
22. Sansam, C. L., and Pezza, R. J. (2015) Connecting by breaking and repairing: mechanisms of DNA strand exchange in meiotic recombination. *FEBS J*. **282**, 2444-2457
23. Tsubouchi, H., and Roeder, G. S. (2002) The Mnd1 protein forms a complex with Hop2 to promote homologous chromosome pairing and meiotic double-strand break repair. *Mol. Cell. Biol.* **22**, 3078-3088.
24. Kang, H. A., Shin, H. C., Kalantzi, A. S., Toseland, C. P., Kim, H. M., Gruber, S., Peraro, M. D., and Oh, B. H. (2015) Crystal structure of Hop2-Mnd1 and mechanistic insights into its role in meiotic recombination. *Nucl. Acids Res.* **43**, 3841-3856
25. Rampler, E., Stranzl, T., Orban-Nemeth, Z., Hollenstein, D. M., Hudecz, O., Schloegelhofer, P., and Mechtler, K. (2015) Comprehensive cross-linking mass spectrometry reveals parallel orientation and flexible conformations of plant HOP2-MND1. *J. Proteome. Res.* **14**, 5048-5062.
26. Zhao, W., and Sung, P. (2015) Significance of ligand interactions involving Hop2-Mnd1 and the RAD51 and DMC1 recombinases in homologous DNA repair and XX ovarian dysgenesis. *Nucl. Acids Res.* **43**, 4055-4066
27. Rockmill, B., and Roeder, G. S. (1991) A meiosis-specific protein kinase homolog required for chromosome synapsis and recombination. *Genes Dev*. **5**, 2392-2404
28. Carballo, J. A., Johnson, A. L., Sedgwick, S. G., and Cha, R. S. (2008) Phosphorylation of the axial element protein Hop1 by Mec1/Tel1 ensures meiotic interhomolog recombination. *Cell* **132**, 758-770
29. Niu, H., Wan, L., Busygina, V., Kwon, Y., Allen, J. A., Li, X., Kunz, R. C., Kubota, K., Wang, B., Sung, P., Shokat, K. M., Gygi, S. P., and Hollingsworth, N. M. (2009) Regulation of meiotic recombination via Mek1-mediated Rad54 phosphorylation. *Mol. Cell* **36**, 393-404
30. Subramanian, V. V., MacQueen, A. J., Vader, G., Shinohara, M., Sanchez, A., Borde, V., Shinohara, A., and Hochwagen, A. (2016) Chromosome Synapsis Alleviates Mek1-Dependent Suppression of Meiotic DNA Repair. *PLoS Biol*. **14**, e1002369
31. Kironmai, K. M., Muniyappa, K., Friedman, D. B., Hollingsworth, N. M., and Byers, B. (1998) DNA-binding activities of Hop1 protein, a synaptonemal complex component from *Saccharomyces cerevisiae. Mol. Cell. Biol*. **18**, 1424-1435
32. Muniyappa, K., Anuradha, S., and Byers, B. (2000) Yeast meiosis-specific protein Hop1 binds to G4 DNA and promotes its formation. *Mol. Cell. Biol*. **20**, 1361-1369
33. Anuradha, S., and Muniyappa, K. (2004) Meiosis-specific yeast Hop1 protein promotes synapsis of double-stranded DNA helices via the formation of guanine quartets. *Nucl. Acids Res*. **32**, 2378-2385
34. Anuradha, S., Tripathi, P., Mahajan, K., and Muniyappa, K. (2005) Meiosis-specific yeast Hop1 protein promotes pairing of double-stranded DNA helices via G/C regions. *Biochem. Biophys. Res. Commun*. **336**, 934-941

35. Tripathi, P., Anuradha, S., Ghosal, G., and Muniyappa, K. (2006) Selective binding of meiosis-specific yeast Hop1 protein to the Holliday junctions distorts the DNA structure and its implications for junction migration and resolution. *J. Mol. Biol.* **364**, 599-611
36. Tripathi, P., Pal, D., and Muniyappa, K. (2007) *Saccharomyces cerevisiae* Hop1 protein zinc finger motif binds to the Holliday junction and distorts the DNA structure: implications for Holliday junction migration. *Biochemistry* **46**, 12530-12542
37. Khan, K., Karthikeyan, U., Li, Y., Yan, J., and Muniyappa, K. (2012) Single-molecule DNA analysis reveals that yeast Hop1 protein promotes DNA folding and synapsis: implications for condensation of meiotic chromosomes. *ACS Nano* **6**, 10658-10666
38. Khan, K., Madhavan, T. P., Kshirsagar, R., Boosi, K. N., Sadhale, P., and Muniyappa, K. (2013) N-terminal disordered domain of *Saccharomyces cerevisiae* Hop1 protein is dispensable for DNA binding, bridging, and synapsis of double-stranded DNA molecules but is necessary for spore formation. *Biochemistry* **52**, 5265-5279
39. Rockmill, B., and Roeder, G. S. (1990) Meiosis in asynaptic yeast. *Genetics* **126**, 563-574
40. Baudat, F., and Nicolas, A. (1997) Clustering of meiotic double-strand breaks on yeast chromosome III. *Proc. Natl. Acad. Sci. U.S.A*. **94**, 5213-5218.
41. Blat, Y., Protacio, R. U., Hunter, N., and Kleckner, N. (2002) Physical and functional interactions among basic chromosome organizational features govern early steps of meiotic chiasma formation. *Cell* **111**, 791-802
42. Smith, A.V., and Roeder, G. S. (1997) The yeast Red1 protein localizes to the cores of meiotic chromosomes. *J. Cell Biol*.**136**, 957-967.
43. Thompson, E. A., and Roeder, G. S. (1989) Expression and DNA sequence of *RED1*, a gene required for meiosis I chromosome segregation in yeast. *Mol. Gen. Genet.* **218**, 293-301
44. Bailis, J. M., and Roeder, G. S. (2000) Pachytene exit controlled by reversal of Mek1-dependent phosphorylation. *Cell* **101**, 211-221
45. Eichinger, C. S., and Jentsch, S. (2010) Synaptonemal complex formation and meiotic checkpoint signaling are linked to the lateral element protein Red1. *Proc. Natl. Acad. Sci. U.S.A.* **107**, 11370-11375
46. de los Santos, T., and Hollingsworth, N. M. (1999) Red1p, a MEK1-dependent phosphoprotein that physically interacts with Hop1p during meiosis in yeast. *J. Biol. Chem.* **274**, 1783-1790.
47. Lin, F. M., Lai, Y. J., Shen, H. J., Cheng, Y. H., and Wang, T. F. (2010) Yeast axial-element protein, Red1, binds SUMO chains to promote meiotic interhomologue recombination and chromosome synapsis. *EMBO J*. **29**, 586-596
48. Schwacha, A. and Kleckner, N. (1997) Interhomolog bias during meiotic recombination: meiotic functions promote a highly differentiated interhomolog-only pathway. *Cell* **90**, 1123-1135
49. Woltering, D., Baumgartner, B., Bagchi, S., Larkin, B., Loidl, J., de los Santos, T., and Hollingsworth, N. M. (2000) Meiotic segregation, synapsis, and recombination checkpoint functions require physical interaction between the chromosomal proteins Red1p and Hop1p*. Mol. Cell. Biol*. **20**, 6646-6658

50. Sen, D., and Gilbert, W. (1988) Formation of parallel four-stranded complexes by guanine-rich motifs in DNA and its implications for meiosis. *Nature* **334**, 364-366
51. Sundquist, W. I., and Klug, A. (1989). Telomeric DNA dimerizes by formation of guanine tetrads between hairpin loops. *Nature* **342**, 825-829
52. Smith, F. W., and Feigon, J. (1992). Quadruplex structure of *Oxytricha* telomeric DNA oligonucleotides. *Nature* **356**, 164-168
53. Williamson, J. R., Raghuraman, M. K., and Cech, T. R. (1989). Monovalent cation-induced structure of telomeric DNA: the G-quartet model. *Cell* **59**, 871-880
54. Venczel, E. A., and Sen, D. (1996) Synapsable DNA. *J. Mol. Biol.* **257**, 219-224.
55. Bergerat, A., de Massy, B., Gadelle, D., Varoutas, P. C., Nicolas, A., and Forterre,P. (1997). An atypical topoisomerase II from Archaea with implications for meiotic recombination. *Nature* **386**, 414-417
56. Keeney, S., Giroux, C. N., and Kleckner, N. (1997). Meiosis-specific DNA double-strand breaks are catalyzed by Spo11, a member of a widely conserved protein family. *Cell* **88**, 375-384
57. West, S. C., Blanco, M. G., Chan, Y. W., Matos, J., Sarbajna, S., and Wyatt, H. D. (2015). Resolution of Recombination Intermediates: Mechanisms and Regulation. *Cold Spring Harb. Symp. Quant. Biol*. **80**, 103-109
58. Dayani, Y., Simchen, G., and Lichten, M. (2011). Meiotic recombination intermediates are resolved with minimal crossover formation during return-to-growth, an analogue of the mitotic cell cycle. *PLoS Genet*. **7**, e1002083
59. Ira, G., Malkova, A., Liberi, G., Foiani, M., and Haber, J. E. (2003). Srs2 and Sgs1-Top3 suppress crossovers during double-strand break repair in yeast. *Cell* **115**, 401-411
60. Matos, J., Blanco, M. G., and West, S. C. (2013) Cell-cycle kinases coordinate the resolution of recombination intermediates with chromosome segregation. *Cell Rep*. **4**, 76-86
61. Szakal, B., and Branzei, D. (2013) Premature Cdk1/Cdc5/Mus81 pathway activation induces aberrant replication and deleterious crossover. *EMBO J*. **32**, 1155-1167
62. Bishop, D. K., Park, D., Xu, L., and Kleckner, N. (1992) *DMC1*: a meiosis-specific yeast homolog of *E. coli* RecA required for recombination, synaptonemal complex formation, and cell cycle progression. *Cell* **69**, 439-456
63. Shinohara, A., Ogawa, H., and Ogawa, T. (1992) Rad51 protein involved in repair and recombination in *S. cerevisiae* is a RecA-like protein. *Cell* **69**, 457-470
64. Friedman, D. B., Hollingsworth, N. M., and Byers, B. (1994) Insertional mutations in the yeast *HOP1* gene: evidence for multimeric assembly in meiosis. *Genetics* **136**, 449-464
65. Schwacha, A., and Kleckner, N. (1997) Interhomolog bias during meiotic recombination: meiotic functions promote a highly differentiated interhomolog-only pathway. *Cell* **90**, 1123-1135
66. Bishop, D. K., Nikolski, Y., Oshiro, J., Chon, J., Shinohara, M., and Chen, X. (1999) High copy number suppression of the meiotic arrest caused by a *dmc1* mutation: *REC114* imposes an early recombination block and *RAD54* promotes a *DMC1*-independent DSB repair pathway. *Genes Cells* **4**, 425-444
67. Xu, L., Weiner, B. M., and Kleckner, N. (1997) Meiotic cells monitor the status of the interhomolog recombination complex. *Genes Dev.* **11**, 106-118

68. Hollingsworth, N. M., Ponte, L., and Halsey, C. (1995) *MSH5*, a novel MutS homolog, facilitates meiotic reciprocal recombination between homologs in *Saccharomyces cerevisiae* but not mismatch repair. *Genes Dev*. **9**, 1728-1739
69. Bailis, J. M., and Roeder, G. S. (1998) Synaptonemal complex morphogenesis and sister-chromatid cohesion require Mek1-dependent phosphorylation of a meiotic chromosomal protein. *Genes Dev.* **12**, 3551-3563
70. Niu, H., Wan, L., Baumgartner, B., Schaefer, D., Loidl, J., and Hollingsworth, N. M. (2005) Partner choice during meiosis is regulated by Hop1-promoted dimerization of Mek1. *Mol. Biol. Cell* **16**, 5804-5818
71. Wan, L., de los Santos, T., Zhang, C., Shokat, K., and Hollingsworth, N. M. (2004) Mek1 kinase activity functions downstream of *RED1* in the regulation of meiotic double strand break repair in budding yeast. *Mol. Biol. Cell* **15**, 11-23
72. van Heemst, D., and Heyting, C. (2000) Sister chromatid cohesion and recombination in meiosis. *Chromosoma* **109**, 10-26
73. Liu, Z., and Gilbert, W. (1994) The yeast *KEM1* gene encodes a nuclease specific for G4 tetraplex DNA: implication of *in vivo* functions for this novel DNA structure. *Cell* **77**, 1083-1092
74. Hershman, S. G., Chen, Q., Lee, J. Y., Kozak, M. L., Yue, P., Wang, L. S., and Johnson, F. B. (2008) Genomic distribution and functional analyses of potential G-quadruplex-forming sequences in *Saccharomyces cerevisiae*. *Nucl. Acids Res*. **36**, 144-156
75. Capra, J. A., Paeschke, K., Singh, M., and Zakian, V. A. (2010) G-quadruplex DNA sequences are evolutionarily conserved and associated with distinct genomic features in *Saccharomyces cerevisiae*. *PLoS Comput. Biol***. 6**, e1000861
76. Gerton, J. L., DeRisi, J., Shroff, R., Lichten, M., Brown, P. O., and Petes, T. D. (2000) Global mapping of meiotic recombination hotspots and coldspots in the yeast *Saccharomyces cerevisiae*. *Proc. Natl. Acad. Sci. U.S.A*. **97**, 11383-11390
77. Marsolier-Kergoat, M. C., and Yeramian, E. (2009) GC content and recombination: reassessing the causal effects for the *Saccharomyces cerevisiae* genome. *Genetics* **183**, 31-38
78. Bochman, M. L., Paeschke, K., and Zakian, V. A. (2012) DNA secondary structures: stability and function of G-quadruplex structures. *Nat. Rev. Genet*. **13**, 770-780
79. Lobachev, K. S., Shor, B. M., Tran, H. T., Taylor, W., Keen, J. D., Resnick, M. A., and Gordenin, D. A. (1998) Factors affecting inverted repeat stimulation of recombination and deletion in *Saccharomyces cerevisiae. Genetics* **148**, 1507-1524
80. Ghosal, G., and Muniyappa, K. (2005) *Saccharomyces cerevisiae* Mre11 is a high-affinity G4 DNA-binding protein and a G-rich DNA-specific endonuclease: implications for replication of telomeric DNA. *Nucl. Acids Res*. **33**, 4692-4703
81. Ghosal, G., and Muniyappa, K. (2007) The characterization of *Saccharomyces cerevisiae* Mre11/Rad50/Xrs2 complex reveals that Rad50 negatively regulates Mre11 endonucleolytic but not the exonucleolytic activity. *J. Mol. Biol*. **372**, 864-882
82. Cahoon, L. A., and Seifert, H. S. (2009) An alternative DNA structure is necessary for pilin antigenic variation in *Neisseria gonorrhoeae. Science* **325**, 764-767
83. Rao, H. B., Qiao, H., Bhatt, S. K., Bailey, L.R., Tran, H.D., Bourne, S.L., Qiu, W., Deshpande, A., Sharma, A.N., Beebout, C.J., Pezza, R.J., and Hunter N.

(2017) A SUMO-ubiquitin relay recruits proteasomes to chromosome axes to regulate meiotic recombination. *Science* **355**, 403-407
84. Ahuja, J.S., Sandhu, R., Mainpal, R., Lawson, C., Henley, H., Hunt, P.A., Yanowitz, J.L., and Börner, G. V. (2017) Control of meiotic pairing and recombination by chromosomally tethered 26S proteasome. *Science* **355**, 408-411
85. Ajimura, M., Leem, S. H., and Ogawa, H. (1993) Identification of new genes required for meiotic recombination in *Saccharomyces cerevisiae*. *Genetics* **133**, 51-66
86. Khan, K., Madhavan, T. P. V., and Muniyappa, K. (2010) Cloning, overexpression and purification of functionally active *Saccharomyces cerevisiae* Hop1 protein from *Escherichia coli. Protein Expr. Purif.* **72**, 42–47
87. Bradford, M. M. (1976) A rapid and sensitive method for the quantitation of microgram quantities of protein utilizing the principle of protein-dye binding. *Anal. Biochem.* **72**, 248-254
88. Sambrook, J., Fritsch, E. F., and Maniatis, T. (1989) Molecular Cloning: A Laboratory Manual, 2nd Edition, Cold Spring Harbor Laboratory Press, Cold Spring Harbor, New York.
89. Duckett, D. R., Murchie, A. I., Diekmann, S., von Kitzing, E., Kemper, B., and Lilley D. M. (1988) The structure of the Holliday junction, and its resolution. *Cell* **55**, 79-89

LEGENDS TO FIGURES

Figure 1. Expression and purification of the Red1 protein. (A) lane 1, protein molecular weight markers; 2, whole cell lysate from uninduced (US) cells (25 µg); 3, whole cell lysate from induced cells (25 µg) ; 4, eluate from Q Sepharose column (8 µg); 5, eluate from Sephadex 200 column (5 µg). (B) Western blot analysis of Red1 using anti-Red1 antibody. Lane 1, purified Red1 protein; 2, pre-stained protein molecular weight markers. In lane 1, the upper band corresponds to the full-length Red1 and the lower band to its proteolytic product.

Figure 2. Protein-protein interaction between Red1 and Hop1. (A) far Western blotting using Red1 as a probe. Increasing concentrations (1 to 5 µg) of purified Hop1 or Rad17 were spotted (from left to right) on nitrocellulose membranes. After incubation with Red1, and blocking, the membranes were probed with anti-Red1 antibody as described under “Experimental Procedures.” (B) A representative SPR sensorgram showing the dose-dependent Red1 binding curves. The data shown is representative of three independent experiments.

Figure 3. Red1 shows structure-selective DNA binding activity. The reaction mixtures from DNA binding assays were subjected to electrophoresis on native polyacrylamide gels as described under Experimental Procedures. Briefly, the reaction mixtures (20 µl) contained 0.5 nM of the indicated ^{32}P-labeled DNA substrate in the absence (lane 1) or presence (lanes 2-11) of 50, 100, 150, 200, 250, 300, 350, 400, 450 and 500 nM Red1 respectively. The triangle on top of the gel image represents increasing concentrations of Red1 incubated with: (A) Holliday junction; (B) 3-way junction; (C) 5' flap; (D) Y

shaped structure; (E) dsDNA; (F) duplex DNA with 3' overhang, and (G) ssDNA. (H) Graphical representation of the extent of Red1 binding to different DNA substrates. The formation of Red1-DNA complexes in panels A to G is plotted versus varying concentrations of Red1. Error bars indicate standard error of the mean (s.e.m.)

Figure 4. Effect of NaCl on the stability of Red1-DNA complexes. The assay was performed with 0.5 nM of the indicated ^{32}P-labeled DNA substrate and saturating concentration of the Red1 protein as described under Experimental Procedures. (A) HJ; (B) 3-way junction and (C) dsDNA. Lane 1, free DNA. 2, DNA-Red1 complex in the absence of NaCl. In lanes 3-12, NaCl was added to a final concentration of 0.1, 0.2, 0.3, 0.4, 0.5, 0.6, 0.7, 0.8 0.9 and 1 M respectively. After 15 min incubation with NaCl, the reaction mixtures were electrophoresed on native polyacrlyamide gels. The gels were dried and exposed to phosphorimager screen. (D) Graphical representation of the extent of dissociation of Red1-DNA complexes in panels A-C plotted versus increasing concentrations of NaCl. Error bars indicate s.e.m.

Figure 5. Red1 fails to promote intermolecular pairing of double-stranded DNA molecules containing a centrally positioned 8 bp G/C sequence. (A) Schematic of the duplex DNA substrate without the G/C sequence. (B) Schematic of the DNA substrate with the centrally embedded 8 bp G/C sequence. Panel C, nucleoprotein complexes with mixed sequence DNA substrates with increasing concentration of Red1. Panel E, nucleoprotein complexes with the substrate containing G/C-rich region with increasing concentration of Red1. The reaction mixtures (20 µl) contained 2 nM ^{32}P-labeled duplex DNA in the absence (lane 1) or presence of 0.2, 0.4, 0.6, 0.8, 1, 1.2, 1.4, 1.6, 1.8 and 2 µM Red1 (lanes 2-11) respectively. In panel D and F, the assay was carried out with 2 nM of the specified ^{32}P-labeled duplex DNA in the absence (lane 1) or presence of increasing Red1 concentration. After 30 min incubation, the reaction mixtures in panel C and E were deproteinized and analyzed as described under Experimental Procedures (panel D and F). The positions of free DNA and the product are indicated on the left-hand side of the image.

Figure 6. Red1 potentiates Hop1 promoted intermolecular pairing of double-stranded DNA molecules containing 8 bp G/C sequence. (A) Schematic of the DNA substrate with the centrally positioned 8 bp G/C sequence. In panel B, the assay was carried out with 2 nM ^{32}P-labeled 48 bp duplex DNA containing 8 bp G/C-rich sequence in the absence (lane 1) or presence of 0.2, 0.3, 0.4, 0.5, 0.6, 0.7, 0.8, 0.9 and 1 µM of Hop1 in lanes 2 to 11, respectively, In panel C, the assay was carried out with 2 nM ^{32}P-labeled 48 bp duplex DNA containing 8 bp G/C sequence in the absence (lane 1) or constant amount (1 µM) of Hop1 (lane 2) and 0.1, 0.2, 0.3, 0.4,0.5,0.6,0.7,0.8,0.9 and 1 µM of Red1 (lanes 3-11) respectively. The reaction mixtures were deproteinized and analyzed as described under Experimental Procedures. The positions of free DNA and the product are indicated on the left-hand side of the image. (D) Graphical representation of the extent of product formed in (B) and (C) plotted verses increasing concentrations of Hop1 alone or Hop1 plus Red1.

Figure 7. DNA sequence specificity of the pairing promoted by Hop1. The reaction mixtures (20 µl) containing 2 nM ^{32}P-labeled DNA incubated in the absence (lane 1) or presence of 1 µM each of Hop1 and Red1 (lane 2). Lanes 3-12 contained1 µM each of Hop1 and Red1 and increasing concentrations of the specified competitor: (A) specific competitor and (B) non-specific competitor. (C) Graphical representation of the decrease in the percentage of Hop1+Red1 mediated pairing in (A) and (B) plotted verses increasing concentrations of the unlabeled DNA.

Figure 8. Red1 promotes bridging of non-contiguous DNA segments into intramolecular stem-loop structures. An aliquot (5 µl) of the reaction mixture was spotted on freshly cleaved mica surface and visualized as described under Experimental Procedures. Panel (A): (i) shows selected AFM images of closed circular plasmid DNA; (ii) to (iv) show images of 5 ng DNA incubated with 100 nM Red1. Panel (B): (i) to (v) show images of 5 ng DNA incubated with 300 nM Red1. The black arrows indicate naked DNA, whereas the green and yellow arrows denote stem-loop or filamentous structures. Panel (C) shows the bar graph of bridged DNA molecules in the presence of indicated concentrations of Red1. Panel (D) shows the percentages of various types of Red1-DNA complexes formed at indicated concentrations of Red1. The numbers on the X-axis correspond to: (1) Red1 binding at random positions; (2) Red1 protein-bound intramolecular DNA nodes; (3) intramolecular stem-loop structures and (4) Red1 nucleoprotein filaments. Vertical bars indicate s.e.m.

Figure 9. Red1 promotes DNA non-homologous end joining. An aliquot (5 µl) of the reaction mixture was spotted on freshly cleaved mica surface and visualized as described under Experimental Procedures. Panel (A) (i) shows AFM image of 2. 6 kb linear duplex DNA incubated in the absence of Red1; plates (ii) to (v), show 5 ng DNA incubated with 100 nM Red1. Panel (B): plates (i) to (iv), show 5 ng DNA incubated with 300 nM Red1. The black arrows denote naked DNA, whereas the green and yellow arrows denote non-homologous DNA end-joining. Panel (C): bar graph depicting the percentage of DNA molecules involved in end-joining promoted by the indicated concentrations of Red1. Vertical bars indicate s. e.m.

Figure 10. Hop1 enhances the Red1 promoted bridging of linear DNA molecules resulting in the formation of linear multimers. Lane 1, DNA ladder marker; 2, 2.6 kb blunt-ended linear double-stranded DNA; lane 3, 2.6 linear dsDNA in the presence of T4 DNA ligase; lane 4, same as lane 3 but incubated with 100 nM Hop1 prior to the addition of T4 DNA ligase; lane 5, same as lane 3 but incubated with 200 nM Red1 prior to the addition of T4 DNA ligase. Lanes 6-9, linear dsDNA was pre-incubated with a constant amount of Red1 (200 nM) in the presence of 200, 250, 300, 350 nM of Hop1 respectively, prior to the addition of T4 DNA ligase. Lanes 10-12, as in lanes 7-9 but the reaction mixtures were incubated with Exo III. The positions of the linear dsDNA and the products formed during the reaction are indicated on the right-hand side of the image.

Table 1. K_d values for the binding of Red1 protein to different DNA substrates. (N.D., not determined)

DNA substrate	K_d (nM)
Holliday junction	65.99 ±1.97
Three way junction	108.2 ±2.57
5’ flap	165.9 ±2.86
Y shaped	526.1 ±6.48
Duplex DNA	115.8 ±4.96
dsDNA with overhang	N.D.
ssDNA	N.D

Figure 1

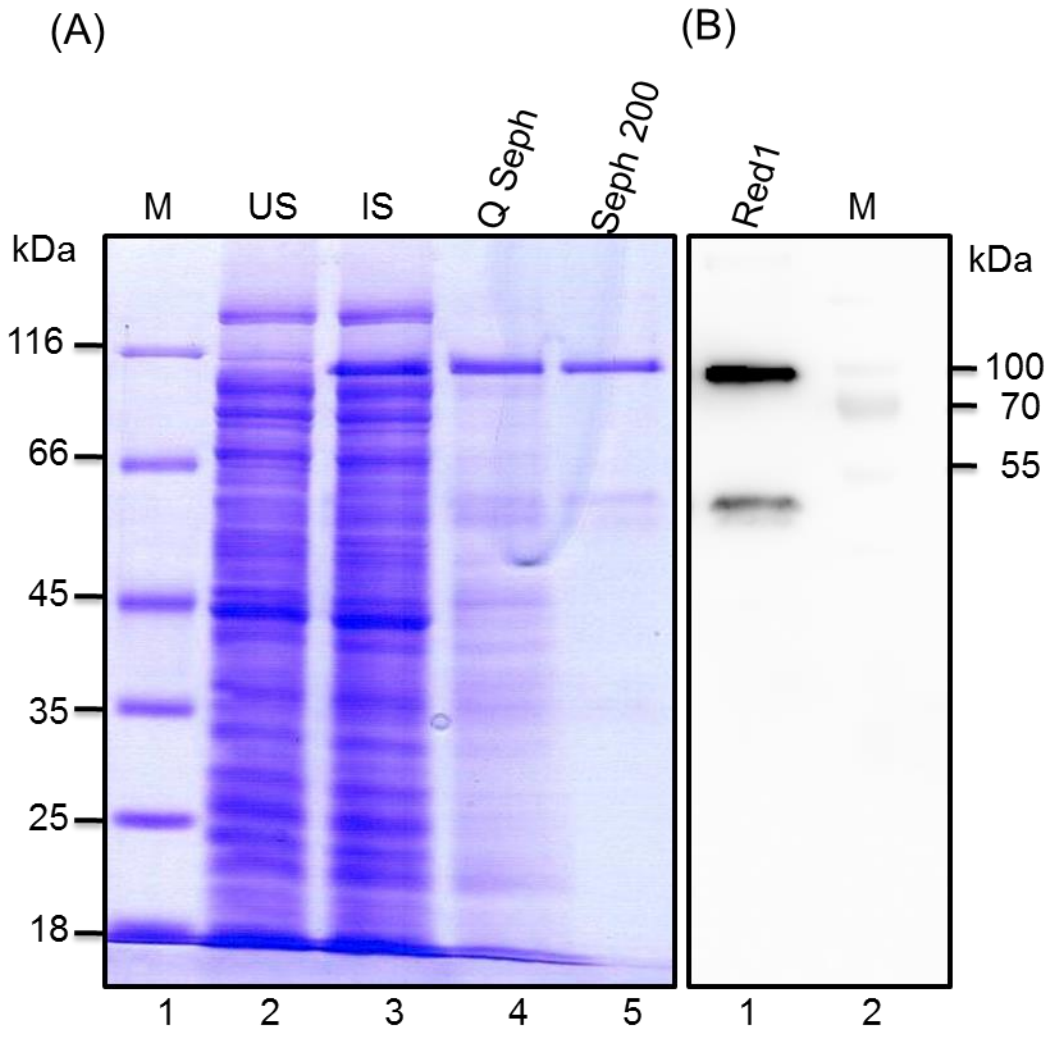

Figure 2

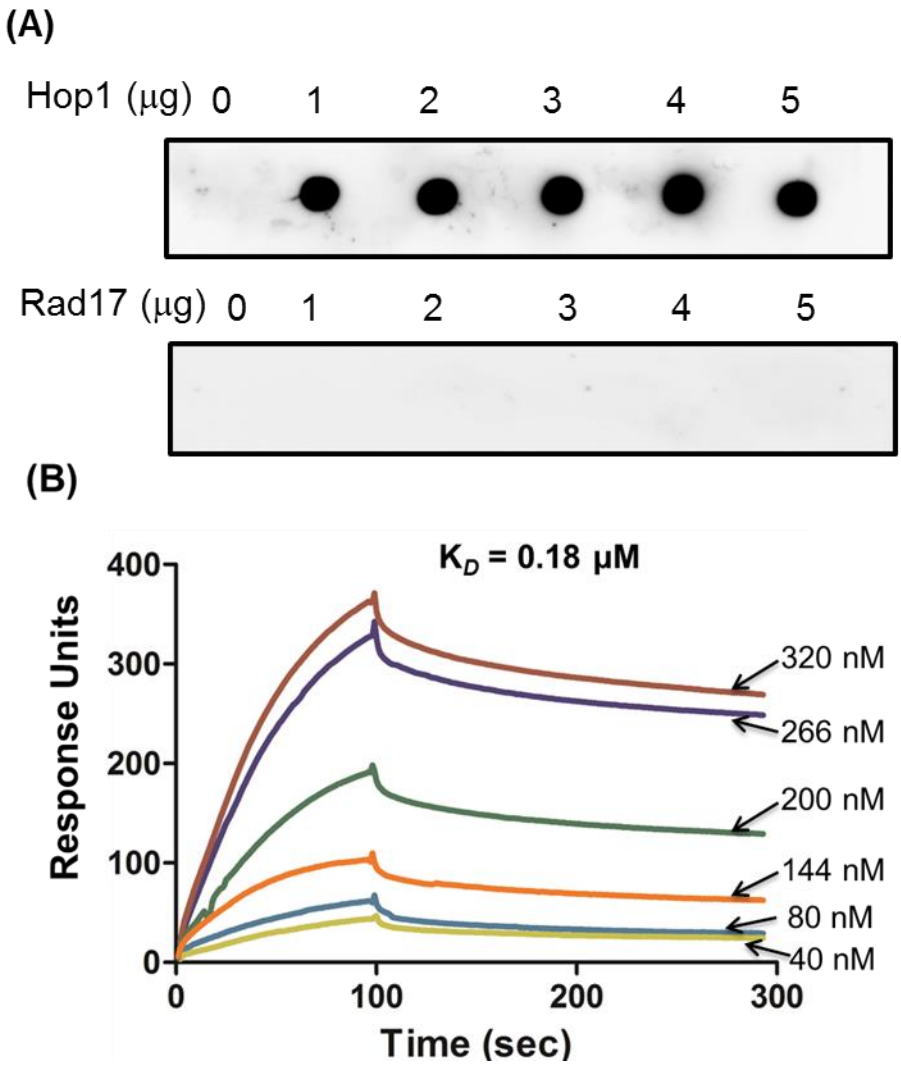

Figure 3

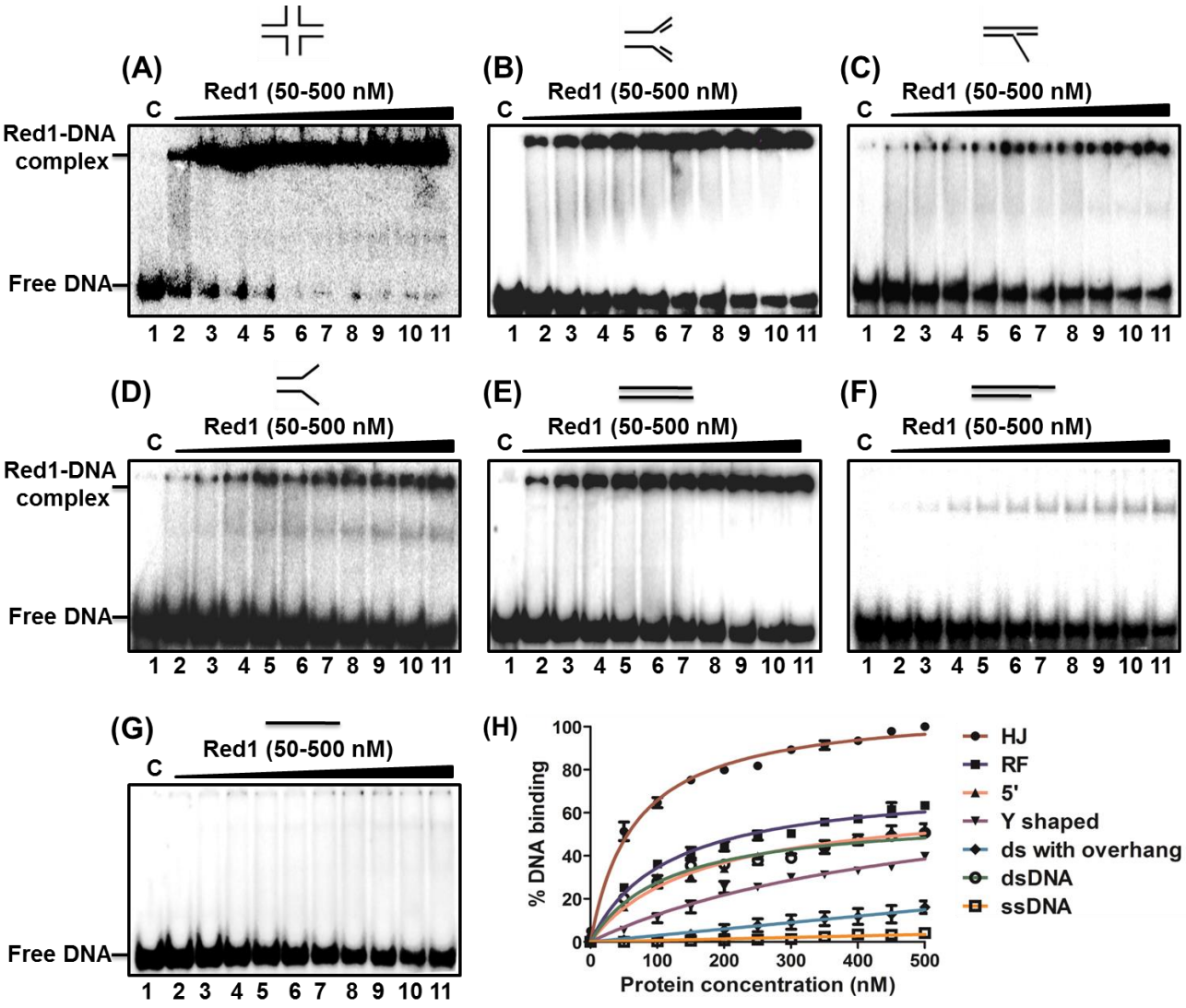

Figure 4

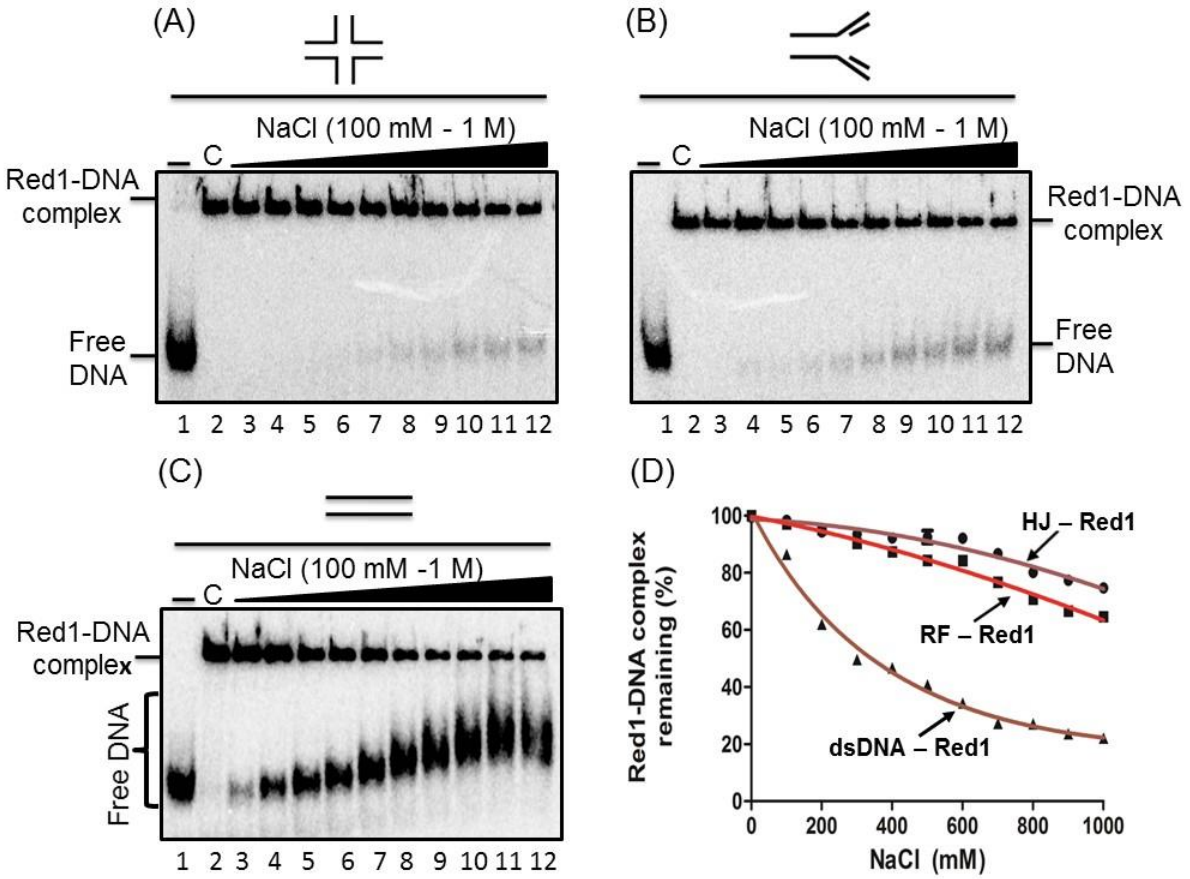

Figure 5

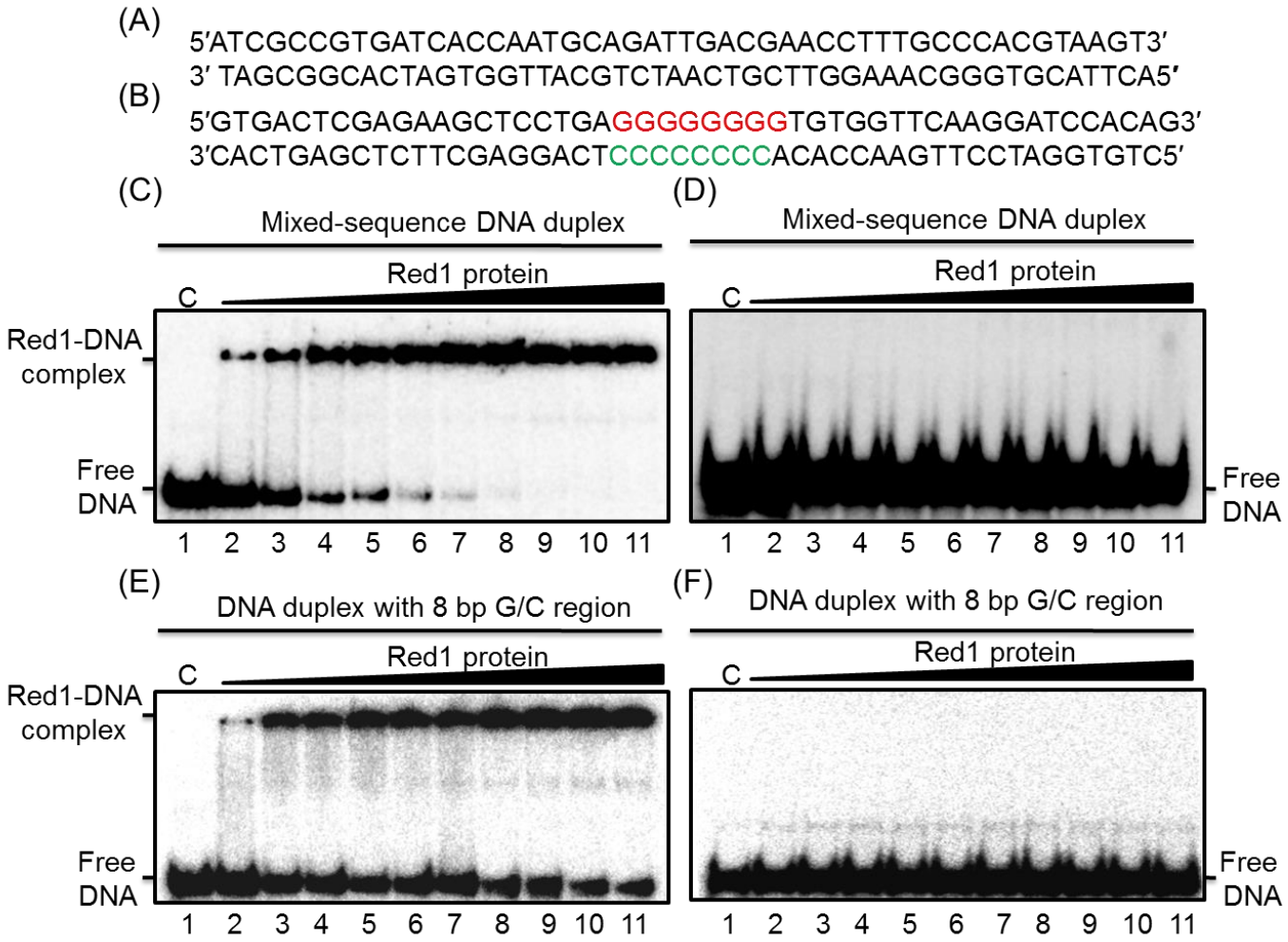

Figure 6

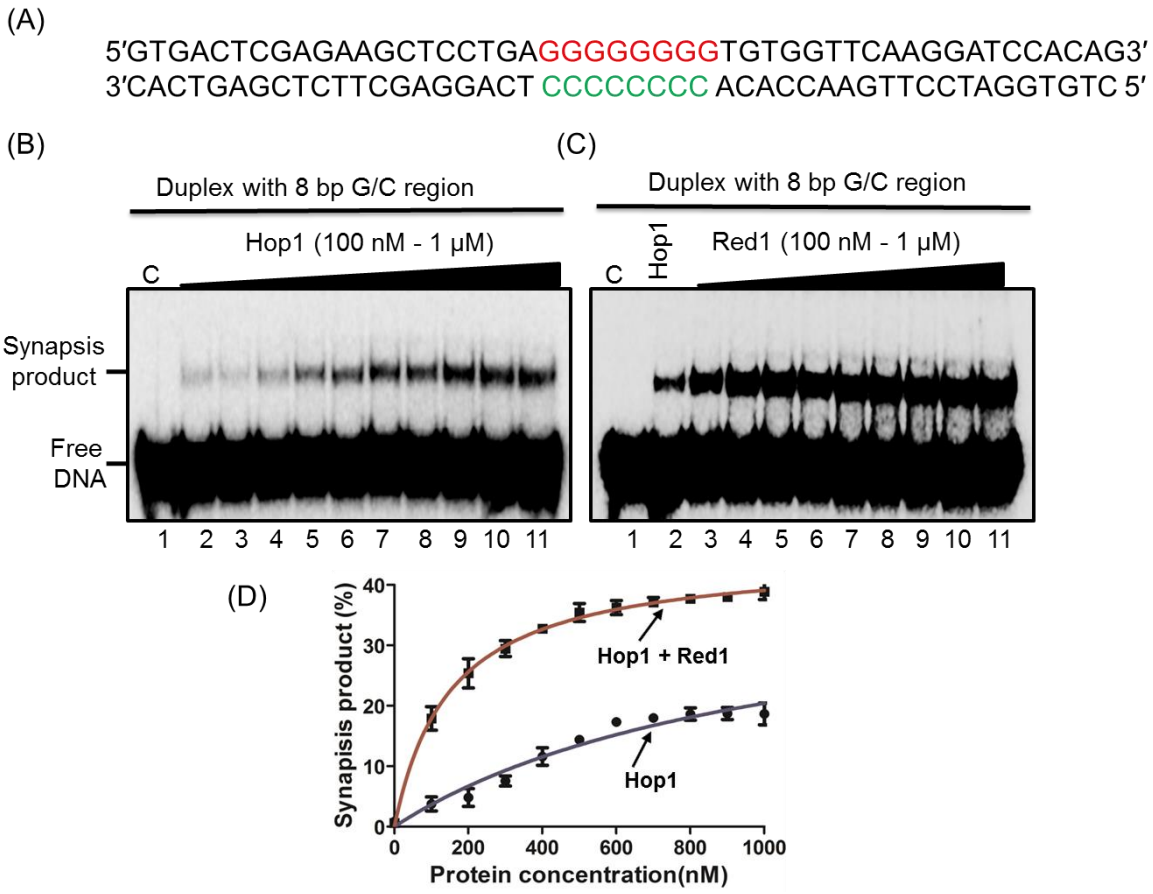

Figure 7

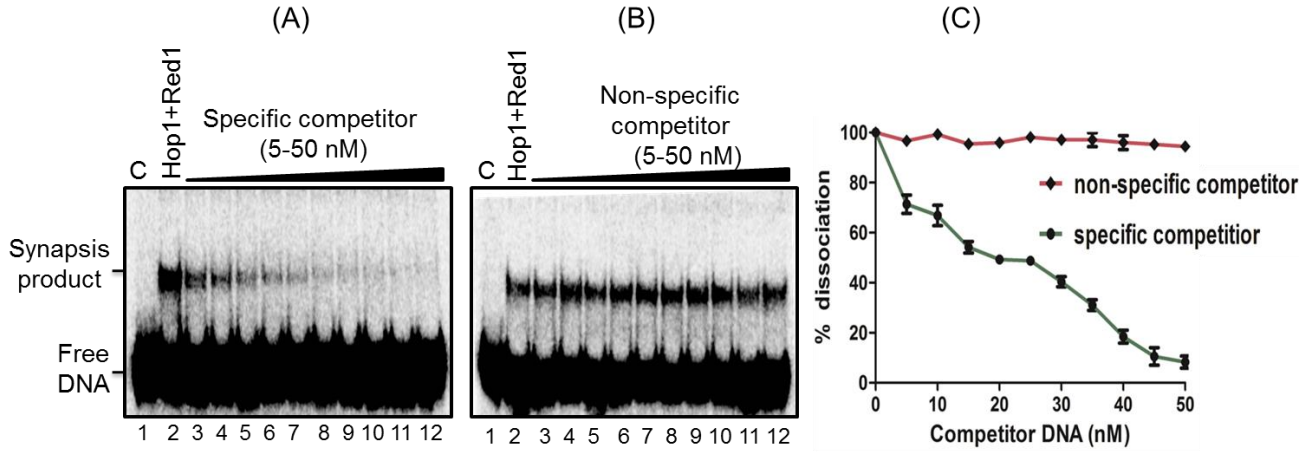

Figure 8

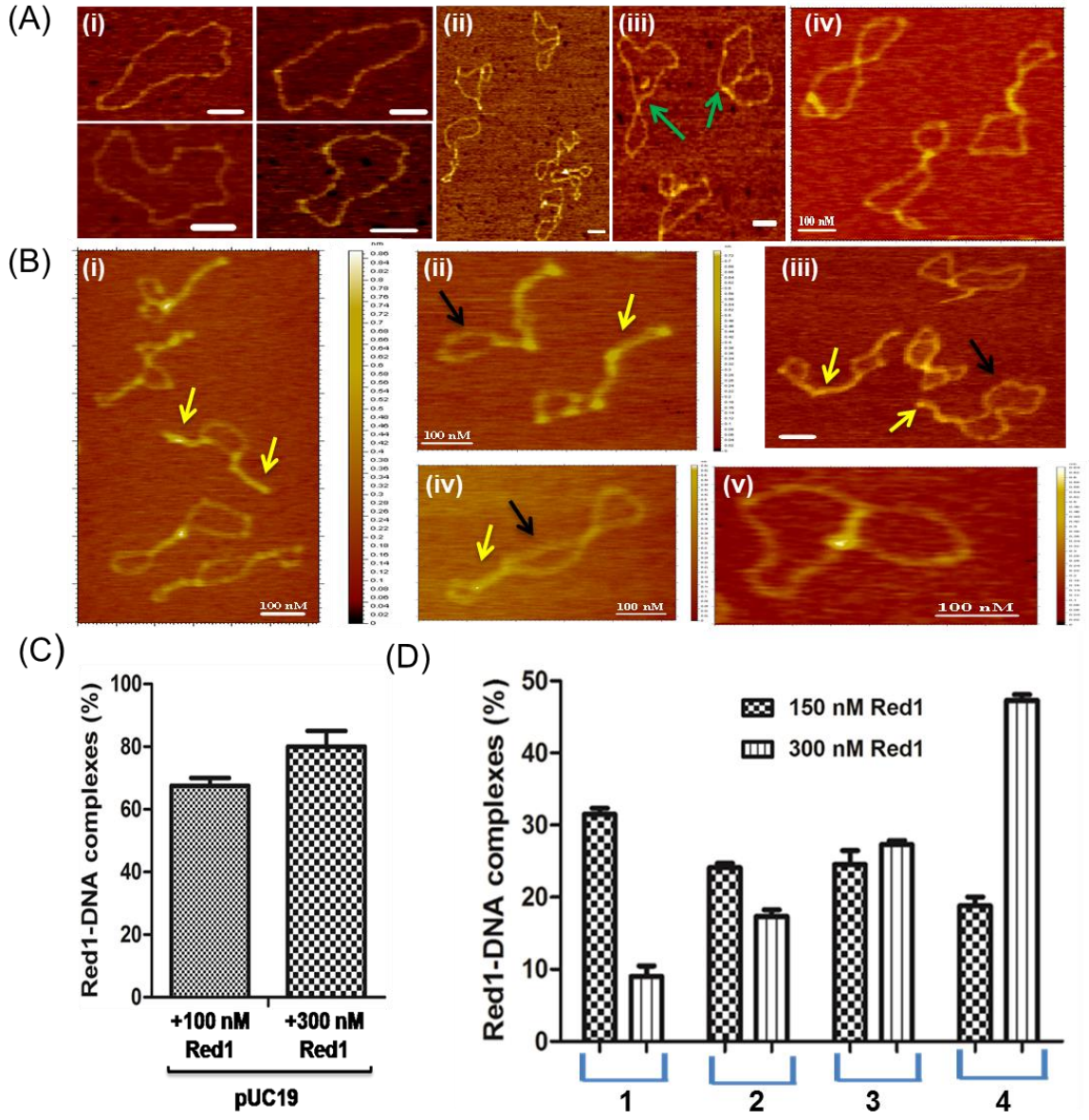

Figure 9

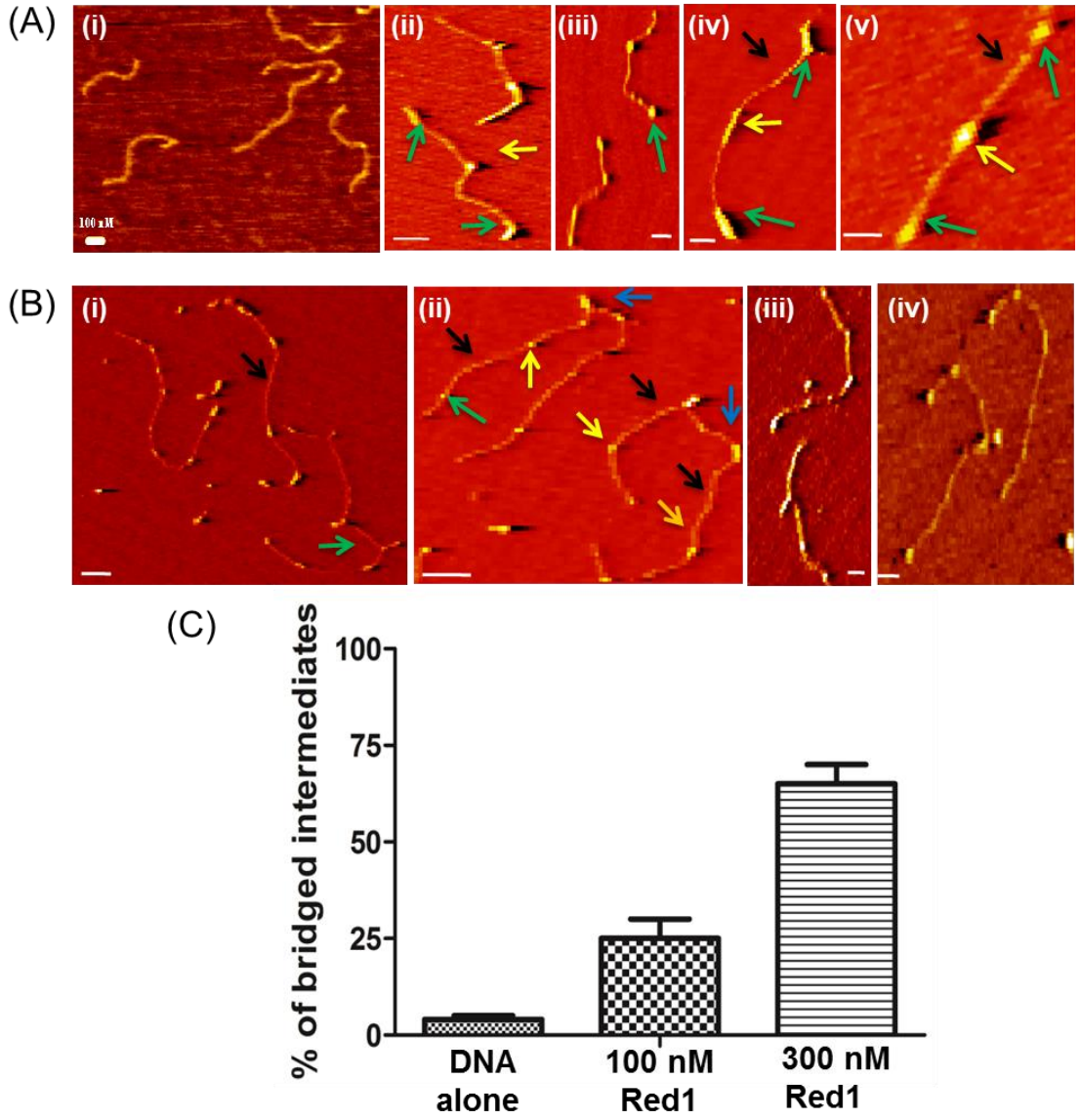

Figure 10

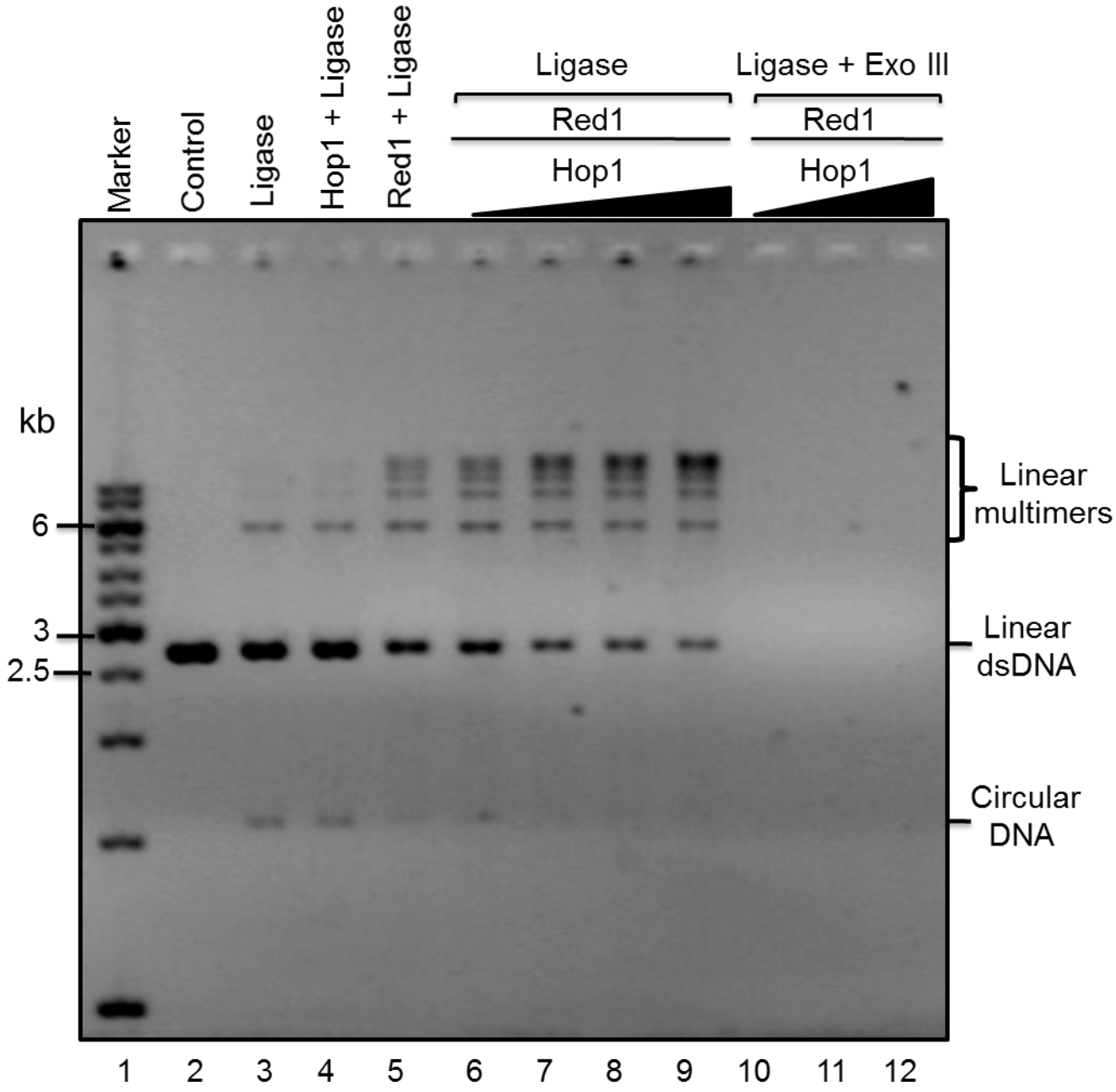

Saccharomyces cerevisiae Red1 protein exhibits nonhomologous DNA end joining activity and potentiates Hop1 promoted pairing of double-stranded DNA

Rucha Kshirsagar, Indrajeet Ghodke and Kalappa Muniyappa

J. Biol. Chem. published online June 22, 2017

Access the most updated version of this article at doi: 10.1074/jbc.M117.796425